TECHNICAL MEMORANDUM

107

Development of the high resolution model

M. Jarraud, A.J. Simmons
and M. Kanamitsu

Research Department

September 1985

European Centre for Medium-Range Weather Forecasts
Europäisches Zentrum für mittelfristige Wettervorhersage
Centre européen pour les prévisions météorologiques à moyen

Acknowledgements

Particular acknowledgement is made to D. Dent for continuing technical development of the model, to C. Branković for work on the climatological fields, to H. Pümpel for synoptic assessment and to J. Steppeler and J-M. Hoyer for the preparation of some of the forecasts. Many other colleagues contributed in some way or other to this work, including the many members of the Operations Department involved in the quasi-operational trials and operational implementation of the model.

E.C.M.W.F.
SCIENTIFIC ADVISORY COMMITTEE
13th SESSION

ECMWF/SAC(85)4
SHINFIELD
7 AUGUST 1985

Subject: Development of the high resolution model

Abstract

A programme of model development and numerical experimentation leading up to the operational implementation of a T106 version of the ECMWF spectral model is described. The technical development necessary to achieve this is summarized first, and an account is then given of the development of highly selective horizontal diffusions which increase the possible timestep by more than 25% with no significant loss of forecast accuracy. A modification to the time-stepping required to enhance computational stability in the planetary boundary layer is also discussed.

The basic experimentation was carried out for 24 cases drawn objectively from a 2-year period and covering all seasons. To aid understanding and place results in a more general context, forecasts were carried out at T21, T42, T63 and T106 resolutions using mean and envelope orographies. Results leading to postponement of consideration of an increase in vertical resolution, and to choices of horizontal diffusion and orographic filtering are first described. This is followed by a more substantial discussion of the orography experiments, highlighting sensitivity to season and resolution and the rôle of different mountain ranges. Evidence for use of an envelope orography is shown to be stronger for T106 than for lower resolutions.

Forecasts exhibit an almost systematic improvement with increasing resolution in the Northern Hemisphere, but no significant overall improvement beyond T42 in the Southern Hemisphere. A tendency for convergence with increasing resolution is apparent in the Northern Hemisphere, but the average improvement from T63 to T106 is far from negligible. Some cases exhibiting substantial synoptic impact are presented, as is an example of an improved precipitation forecast. Mean forecast errors are briefly discussed.

Results from further pre-operational testing are also presented, although the significance of some of these is open to question. In particular, a quasi-operational trial lasting a little over one month, although indicating some benefits from the use of higher resolution and new parameterizations, gave poorer results than previous experimentation had suggested would be the case. This is thought to be due to the particular synoptic situation prevailing during the period of the trial.

CONTENTS

1. INTRODUCTION

A major revision of the operational ECMWF spectral forecast model was implemented on 1 May 1985. The horizontal resolution of the model's representation of upper-air fields was increased to a triangular truncation at total wavenumber 106 (T106), and revised, higher resolution surface fields were introduced. Included in the latter was an 'envelope' orography based on a spectral fit to a grid-square mean orography enhanced by one standard deviation of the sub grid-scale orography. Substantial changes to the parameterization were also made, with the introduction of a representation of shallow convection, a substantial modification of the deep convection scheme, a new treatment of clouds, and changes to the description of large-scale condensation. The horizontal diffusion was modified to enhance stability and allow use of a longer (15 minute) timestep than would otherwise have been possible, and the model calculation was adapted to make simultaneous use of the two processors of the Centre's CRAY X-MP computer. The parameterization changes are the subject of a companion paper (ECMWF/SAC/(85)5); an account of the other changes and the experimentation leading up to them is the principal subject of this report.

Most of the results discussed here were obtained from a major experimental programme carried out over a period of about one year following acceptance of the CRAY X-MP/22. The main objective of this programme was to make an appropriate choice of resolution, orography and other model parameters for a revised operational model making optimum use of the features of the X-MP/22. However, it was recognized at the planning stage that this was an ideal opportunity to investigate more generally the sensitivity of forecast quality and model behaviour to horizontal resolution and the representation of orography. Experimental forecasts using mean and envelope orographies were thus carried out at T21 and T42 resolutions, at the (previous) operational (T63) resolution, and the proposed T106 resolution. The lower resolution experiments have helped understanding of the higher resolution results, and provide a basis for future model development, which in its initial experimental phase will typically involve forecasts at less than the full operational resolution. These experiments may also be of some more widespread relevance for general circulation modelling.

Most results presented here are from controlled experimentation using a sample of 24 cases drawn from all seasons. Prior to operational implementation, the high resolution model was run in a continuous quasi-operational data assimilation starting from 12Z 26 March 1985. Ten-day forecasts were performed every two days from 27 March to 10 April, and daily thereafter. Some results from this test of the complete changes, and first impressions of the subsequent operational forecasts, are included later in the paper.

This introductory section is followed by sections discussing aspects of technical development and the time-stepping changes. Section 4 then outlines the overall design of the experimental programme. A justification of some early choices is given in Section 5, which is followed by sections dealing with the sensitivity of forecasts to orography and horizontal resolution. Some results concerning extended integrations, other surface fields, data assimilation, and the final quasi-operational tests are presented in Section 8. Concluding remarks are given in Section 9.

2. TECHNICAL DEVELOPMENT

The technical work required to develop the high resolution model to a stage suitable for quasi-operational testing and subsequent implementation falls naturally into three areas:

(a) Optimization of the model and related post-processing.

(b) Incorporation of the model in the data assimilation.

(c) Production of high resolution surface climatologies.

Major progress in the first of these topics, particularly with regard to the use of the Solid-State Storage Device (SSD) for Input/Output and the production of a dual-tasking version of the model, was reported to last year's meeting of the SAC.

Significant effort has continued to be devoted to optimization of the model. The efficiency of the I/O and dual tasking has been examined and enhanced, and further savings have resulted from revisions of the basic code. Taken together with the timestep change discussed in the following section, this has resulted in a reduction of more than 40% in the cost of a ten-day forecast with post-processing at T106 L16 resolution, and has enabled this resolution to be adopted operationally. The present operational model on the CRAY X-MP/22 requires about the same proportion of available computational resources as did the former operational models on the Cray-1.

The post-processing has been extended to provide output not only in the Cyber format used for dissemination and archiving, but also in the new GRIB code adopted for MARS (see ECMWF/SAC/(85)9). A complete operational archive at the full resolution of the model is now being accumulated using MARS; the Cyber archiving continues at T63 resolution for upper-air fields, although surface fields are kept at full resolution. A multi-tasking version of the post-processing has also been developed, but has not been implemented as post-processing strategy is to be reassessed in the light of experience with the X-MP/48 computer.

In planning the implementation of a complete high resolution forecasting system it was recognized that the high resolution model would be ready for operational use some time before the new analysis code would be developed to the point of providing a higher resolution analysis. It was thus decided to implement the higher resolution model in the data assimilation cycles, using existing interface code to provide a first guess on the regular N48 grid of the original operational analysis and to interpolate upper-air analysis increments from this grid to the grid of the high-resolution model. The analysis of surface parameters was, however, adapted directly to the high-resolution grid. The work involved in this implementation was in principle straightforward, but a number of practical problems arose. It was decided not to seek efficient solutions which would become redundant with the development of the new analysis system. Thus, while the incorporation of higher resolution in the data assimilation was well tested technically, a body of experimentation sufficient to quantify the benefits of this aspect of the resolution increase could not be undertaken.

The final major area requiring technical development was the system for producing climatological surface information on the grid of the model, for use in the surface data analysis and in the forecast. This had previously involved running a sequence of separate programs which had evolved as the forecasting system changed over the past six years, and all of which produced fields on the N48 grid of the Centre's original operational model. Data were subsequently interpolated to the grid of the spectral model. Software has now been developed to facilitate the production of fields at user-defined resolutions directly from the grids of the basic climatological data. As a by-product, a number of errors and inconsistencies in the original procedures have been corrected, and a number of deficiencies in the basic source data have been identified. The work involved was such that the new climatological fields were not available for the bulk of testing of the high resolution model.

3. MODIFICATIONS TO TIME-STEPPING SCHEMES

3.1 Changes in horizontal diffusion to enable use of longer timesteps

Experience with both operational and research forecasting has revealed two situations which predominantly limit the time-step possible in the model. The first is the occurrence of a strong polar-night jet in the statosphere during late winter in the Southern Hemisphere. The second is a strong tropospheric jet stream over the Western Pacific during the Northern Hemisphere winter. The former has resulted in operational failure and use of a shorter time-step during the August-October period for each year since 1981. Moreover, in tests of 20 cases at T106 L16 resolution, two forecasts became unstable using a 12-minute timestep. One involved the first situation, and the other the second. A further example involving the second occurred in a test of the high resolution model in data assimilation.

Two modifications to the horizontal diffusion have been developed to enable use of longer timesteps in these situations. The first entails a general substantial increase in horizontal diffusion for the smallest scales at upper model levels. For each level k, a critical total wavenumber n_k is defined. The standard coefficient K of fourth-order horizontal diffusion is then used for $n \leqslant n_k$, while for $n > n_k$ the value Kh^c is used, where c is the number of levels ℓ (below and including k) such and $n_\ell < n$. The values chosen for testing and operational implementation of the T106 L16 model are, h = 10 and

n_k 84, 88, 92, 96, 100, 103, 105, 106, ...106 for

k = 1, 2, 3, 4, 5, 6, 7, 8,.....16.

This effectively acts as a slight reduction in model resolution at stratospheric levels, without generating the noise found in tests in which the highest-wavenumber components were simply set to zero at these levels.

The second modification involves increased damping at model levels where the maximum wind exceeds a critical value. For a particular model level, spectral components whose total wavenumber n exceeds a critical value n_{crit} (which

depends on the maximum windspeed at that level) are damped at the timestep in question by a factor

$$1 + \alpha \frac{\Delta t}{a} [\mathrm{Max}\{|\underset{\sim}{u}|\}](n-n_{crit})$$

where Δt is the timestep, a the radius of the earth, $\underset{\sim}{u}$ the horizontal velocity field at the particular level, and

$$n_{crit} = \beta/\mathrm{Max}\{|\underset{\sim}{u}|\}$$

Values $\alpha \geq 2$ and $\beta = a/\Delta t$ are sufficient to avoid exponential computational instability for the linear advection equation for a wave of scale a/n and advecting velocity $\mathrm{Max}\{|\underset{\sim}{u}|\}$. In the model, β is defined through a critical velocity, V_{crit}:

$$\beta = V_{crit} \frac{\Delta t_o n_o}{\Delta t}$$

where Δt_o = 1200s and n_o = 63. Here V_{crit} corresponds to a critical velocity for stability (with α=0) for a T63 model with a 20 minute timestep. The values α = 2 and V_{crit} = 90 m s^{-1} were used in the initial tests of the scheme at T106 resolution, but gave one case which, though stable, exhibited transient noise at the level of the tropospheric jet for a 15-minute timestep. The choices α = 2.5 and V_{crit} = 85 m s^{-1} were made for final testing and operational implementation. This is equivalent to setting β = 1.009a/Δt.

The above changes were extensively, but separately, tested at T63 resolution, and found to offer the possibility of a timestep increase of 30% or more with negligible loss of accuracy. Testing of a combination of the changes was thus carried out at T106 resolution using a 15-minute timestep. Three cases were examined using the values α = 2 and V_{crit} = 90 m s^{-1}, and stable integrations were carried out to day 10 in each. Included was the case of 15 January 1984, for which the standard high resolution forecast became unstable beyond day 9 with Δt = 12 minutes. The objective verification presented in Fig. 1 shows the impact of the change in diffusion and timestep to be small compared with that of the change from T63 to T106, and this is confirmed by subjective evaluation of the forecasts. An example in terms of 5-day mean 500 mb height maps for an instance of distinct sensitivity to resolution is presented in Fig. 2.

As noted above, the values $\alpha = 2.5$ and $V_{crit} = 85$ m s^{-1} were chosen for subsequent use. This small further change was first tested in conjunction with a change in the value of the coefficient of horizontal diffusion for divergence, and experimental results showing the impact of the change in α and V_{crit} alone are thus unavailable. All evidence, however, suggests that any impact must have been extremely small. Rather than presenting further conventional synoptic maps, we show in Fig. 3 maps of the 250 mb relative vorticity for three day 9 forecasts from 15 January 1984. One is a T106 forecast with a 15 minute timestep using the new values of α and V_{crit} and a diffusion coefficient of 2.5×10^{15} m^4 s^{-1} for divergence, one a standard ($h=1$, $\alpha=0$) T106 with 12 minute timestep and diffusion coefficient of 5×10^{15} m^4 s^{-1}, and one a standard T63 integration. The 250 mb level is close to the level at which the wind reached a relatively high maximum speed of around 100 m s^{-1} at this stage of the model runs, causing computational instability a few hours later in the standard T106 integration using $\Delta t =$ 12 minutes. The region shown in Fig. 3 is one for which the synoptic-scale evolution was not particularly sensitive to resolution. The figure shows how both higher resolution forecasts produce distinctly sharper gradients in the vorticity field, with no indication of any substantial weakening of gradients due to the use of selective damping in the forecast with 15 minute timestep. In view of such results, the modifications to the horizontal diffusion have been used (so far successfully) for all T106 forecasts carried out over the past six months or so.

3.2 Modification of the time-stepping in the parameterization of vertical diffusion

Detailed evaluation of the results of integrations at T106 resolution revealed a marked tendency for noise to develop in the model boundary layer in regions of strong low-level flow. Examination of corresponding T63 forecasts showed a rather similar noise, but of weaker amplitude, and of a larger horizontal scale that could on occasions be confused with small synoptic-scale variations. Apparently similar problems with derivatives of the ECMWF model have been reported by Larsson (personal communications) using a single column version and by Källberg and Gollvik using a limited-area model based on the Centre's original grid-point model. Thenoise was ascribed to a time-stepping problem in the case of strong vertical diffusion, and a solution was found by utilizing shorter timesteps for this parameterization. This has the disadvantage of increased computational cost.

An efficient remedy to the problem has been found by modifying the time-scheme used to solve the vertical diffusion equation. Writing this equation in the general form

$$\frac{\partial \Psi}{\partial t} = \frac{1}{\rho}\frac{\partial}{\partial z}\left(\rho\ K(\psi)\ \frac{\partial \psi}{\partial z}\right) ,$$

the tendency due to vertical diffusion was computed in the model as $(\psi^*(t+\Delta t) - \psi(t-\Delta t)) / 2\Delta t$, where

$$\frac{\psi^*(t+\Delta t)-\psi(t-\Delta t)}{2\Delta t} = \frac{1}{\rho}\frac{\partial}{\partial z}\left(\rho\ K(\psi(t-\Delta t))\ \frac{\partial}{\partial z}\psi^*(t+\Delta t)\right).$$

The solution comprised replacing the $\psi^*(t+\Delta t)$ on the right-hand side of this equation by $1.5\psi^*(t+\Delta t) - .5\psi(t-\Delta t)$. It was suggested by examining the simpler equation

$$\frac{\partial x}{\partial t} = - k|x|x + f$$

for constant k and f. Evaluating $|x|x$ as $|x(t-\Delta t)|x(t+\Delta t)$ yields a solution which oscillates about $\sqrt{\frac{h}{k}}$ with a period $4\Delta t$ in the limit as $\sqrt{(fk)}\ \Delta t \to \infty$. With $x(t+\Delta t)$ replaced by $\gamma x(t+\Delta t) + (1-\gamma)x(t-\Delta t)$, the oscillation is damped by a factor $\frac{2-\gamma}{\gamma}$ each timestep for $\gamma > 1$. Tests in the full model with $\gamma = 1.25$, 1.5 and 2 showed the first value to be insufficient to control fully the noise. Very similar results were obtained with the other two values, the smaller one being chosen as it gives a smaller truncation error for weak diffusion coefficients.

An example of the impact of the change on one of the disseminated ECMWF products, the wind extrapolated to a 10 m height from the lowest level of the model, is shown in Fig. 4. Illustrated are three two day forecasts for a case of strong southwesterly flow over the central North Atlantic Ocean. The T106 forecast with the former time-stepping for the vertical diffusion equation clearly exhibits a sequence of maxima and minima in wind strength, and some indication of this is perhaps also evident in the corresponding T63 forecast. The new scheme clearly gives a much more uniform low-level flow, and vertical structure in the boundary layer is similarly improved.

This change was developed immediately prior to the quasi-operational testing of the T106 model, and was unavailable for the bulk of the high-resolution experimentation reported later in this paper. However, the results of experimentation such as shown in Fig. 4 indicate that the change has a relatively small impact on the synoptic and larger-scale evolution of the forecast.

4. DESIGN OF THE EXPERIMENTAL PROGRAMME

Plans for the basic experimental programme were presented to the SAC last year. These called for a first experimental phase comprising forecasts from 12 objectively chosen cases, namely the 15th of each month from May 1983 to April 1984. It was anticipated that a number of choices concerning the configuration of the higher resolution model would be made on the basis of results from some or all of theses cases, with particular emphasis on the May, July, October and January forecasts. Discussion of these choices is given in the following section.

Results from the first 12 cases exhibited some marked seasonal variations, and in particular raised questions concerning the performance of the envelope orography in summer. In addition, all cases had been chosen from dates prior to a major change in the operational analysis system used to produce initial conditions. It was thus decided to continue the programme by running forecasts from the 15th of each month from May 1984 onwards. With a subsequent need to perform tests using new parameterization schemes, the series was eventually extended to 24 cases spanning the two year period up to April, 1985.

Forecasts for all 24 cases were carried out using 4 horizontal resolutions - T21, T42, T63 and T106 - and for mean and envelope orographies. The envelopes were based on adding $\sqrt{2}$ standard deviations of the sub grid-scale orography to the mean; in addition, a set of T106 forecasts was carried out using a lower envelope based on adding one standard deviation.

It would have been quite impractical to perform data assimilation for all cases, resolutions and orographies. Initial conditions were thus in each case based on the operational T63 analyses produced using one or other of two versions of the $\sqrt{2}$ standard deviation envelope orography. Analyses produced using the earlier version operational until February 1984 were converted to the later version for the purpose of these experiments. Upper-air fields were formed by spectral fits of fields which had been vertically interpolated from one set of coordinate surfaces to the other at each point of the model's Gaussian grid. Similar procedures were used to produce the T63 mean-orography initial data, and all the T106 datasets, using T106 mean and envelope orographies created using the higher resolution Gaussian Grid. Upper-air fields, surface pressures and orographies for the T42 and T21 experiments

were obtained directly by truncation of T63 fields. All other surface fields, for all resolutions and orographies, were derived by simple linear interpolation from the operational T63 initial conditions. These procedures, together with use of the operational T63 analyses for verification, inevitably introduce some bias in favour of T63 resolution and envelope orography, but available evidence indicates that this is not enough to invalidate the conclusions presented here. However, the use of T63 surface fields means that these cases cannot be used to gain a comprehensive picture of the influence of higher resolution on forecasts of surface and near-surface parameters.

For each particular initial date the same model parameters and parameterizations were used for all resolutions and orographies, with the exception of the horizontal diffusion coefficient. T63, T42 and T21 forecasts all used the operational T63 values of 2×10^{15} m^4 s^{-1} for vorticity, temperature and humidity, and 2×10^{16} m^4 s^{-1} for divergence. For reasons discussed in the next section, the value 10^{15} m^4 s^{-1} was chosen for all variables for the first 19 cases run at T106 resolution. The coefficient for divergence was increased to 2.5×10^{15} m^4 s^{-1} for the final five cases. The parameterizations used for all forecasts for these five cases included the FESFT radiation scheme used operationally since December 1984 and the new treatments of clouds, convection and large-scale condensation introduced operationally with the change of resolution. The forecasts for the other cases used one or other of the two slightly different versions of the parameterization schemes that were used operationally between May and December, 1984.

Selected cases from within the sample of 24 were chosen for further experimentation, such as the tests of time-stepping changes that have already been discussed. A small number of forecasts were also run from other operational or FGGE analyses of special interest, but did not yield results of sufficient novelty to justify presentation here. The final phase of experimentation comprised the quasi-operational testing mentioned in the Introduction.

5. JUSTIFICATION OF EARLY CHOICES

5.1 The combination of horizontal and vertical resolution

This choice was thought likely to be largely independent of the others to be made, and was thus investigated first. Potential operational combinations on the X-MP/22 included T106 with the same 16-level resolution as used previously and T95 with a 20-level resolution. Previous tests had shown no consistent improvements to result from increases in vertical resolution in the boundary-layer or high stratosphere, so study was made of the impact of a 20-level resolution in which layer thicknesses in the middle and upper troposphere were reduced by a third. Results of 4 forecasts (carried out at T63 horizontal resolution) were reported in to the SAC last year, and 4 further cases were subsequently examined. The latter confirmed the earlier conclusion, namely that the increased resolution gave slightly worse results at both 500 and 1000 mb, as shown in the mean objective scores presented in the left-hand plots of Fig. 5. The deterioration was more evident in the winter cases, and over the European and Mediterranean areas as shown also in Fig. 5. It must be stressed that the sample is small, particularly for drawing reliable conclusions as to seasonal or regional performance. However, taking into account the independent development of finite-element schemes for the vertical representation, it was decided to postpone further investigation of vertical resolution until it could be carried out in conjunction with comprehensive testing of the finite-element approach, including study of the interaction with parameterization schemes. Attention was thus concentrated on an increase in horizontal resolution.

5.2 Horizontal diffusion

The sensitivity of medium-range forecasts to the choice horizontal diffusion is such that some early experimentation was required to make a first decision on this choice. The four basic cases were examined at T106 horizontal resolution using the usual ∇^4 diffusion with three different coefficients (applied to all prognostic upper-air variables). The values were 2.5×10^{14} m^4 s^{-1}, corresponding to the same e-folding time on wavenumber 106 as given by the then operational 2×10^{15} m^4 s^{-1} on wavenumber 63, 1×10^{15} m^4 s^{-1} and 2×10^{15} m^4 s^{-1}. Objective and subjective verification clearly indicated a non-negligible deterioration when using the lowest value. Differences between 10^{15} and 2×10^{15} m^4 s^{-1} were much smaller, and (due to the small sample) most likely insignificant. The preliminary choice of 10^{15} m^4 s^{-1} was thus made to minimize any masking of model deficiencies.

Further experimentation and more detailed synoptic assessment indeed revealed some problems. In certain convectively unstable situations, interaction between the dynamics and parameterization produced excessively strong vertical velocities and evident noise in the low-level pressure and temperature fields (Figs. 6a and 6b). Also, apparently spurious wavetrains of strong vertical velocity sometimes developed in situations with strong jets or horizontal gradients of temperature. This led in the operational T63 model to an increase by a factor of 10 in the horizontal diffusion of divergence, as reported last year. In the absence of a better immediate alternative, a similar (though more modest) solution was sought for T106. Increasing the diffusion by a factor of 5 proved quite successful at controlling noise (Fig. 6c), but had a slight detrimental effect on the synoptic scale quality of the forecast. Limited experiments with a ∇^8 diffusion showed a similar effect. Pending further investigation, the ∇^4 scheme with coefficient of 10^{15} m^4 s^{-1} for vorticity, temperature and humidity and 2.5×10^{15} m^4 s^{-1} for divergence, was chosen for final testing and operational implementation.

5.3 Gaussian filtering of the orography

A truncated spectral representation of the earth's orography inevitably exhibits ripples over the ocean, particularly in the vicinity of steep mountains. Although probably of little importance for the large-scale dynamics, particularly at higher resolution, these ripples tend to act as small hills, and can trigger noticeable biases in the patterns of precipitation. Amplitudes can reach several millimetres per day.

To minimize this, the effect of applying a weak filter prior to the spectral fitting of the orography was investigated. The filter was a bi-dimensional Gaussian one similar to that used in the ECMWF N48 grid-point model, but with a radius of 50 rather than 100 km. This produced a quite significant reduction in ripples at the expense of a slightly poorer least-squares fit to the original unsmoothed orography. Testing on the four basic cases gave most satisfactory results, with a negligible impact on the synoptic-scale forecasts, as in the day 10 maps of 1000 mb height shown for one case in Fig. 7, but with a clear reduction in the spurious "orographically-induced" precipitation over the oceans. This filtering was thus used for all subsequent T106 forecasts.

6. OROGRAPHY EXPERIMENTS

6.1 Introduction

The $\sqrt{2}$ standard-deviation envelope orography was introduced into operational forecasting along with the spectral model in April, 1983. Diagnostic studies reported by Wallace et al. (1983) had previously indicated an inadequate orographic forcing in the then operational grid-point model, and significant improvements in medium-range forecast quality were obtained for two winter periods using a 2 standard-deviation envelope with this model (Wallace et al., loc. cit.; Tibaldi, 1985). Subsequent limited pre-operational experimentation using 1, $\sqrt{2}$ and 2 standard-deviation envelopes in the spectral model produced similar results (Simmons and Jarraud, 1984). However, as in the previous experimentation, a slight worsening of short-range forecasts was found, and no comprehensive assessment was carried out for summer situations. A number of local problems in connection with the use of data and forecast products in mountainous areas were also evident. This motivated the re-assessment of the sensitivity of forecasts to orographic representation undertaken as part of the development of the high resolution model.

6.2 Objective verification for the Northern Hemisphere

As anticipated on the basis of preliminary T63 forecasts reported to the 1984 session of the SAC, results indeed showed a striking seasonal sensitivity. The 24 cases have thus been divided into two groups of 12, one broadly representing winter (November to April) and one summer (May to October), the division of spring and autumn months being based on diagnosis of the annual cycle (Volmer et al., 1983). Objective verification here, as elsewhere in this paper, is for simplicity based on anomaly correlations, although results have been confirmed by examination of standard deviations.

Mean differences between 500 mb height anomaly correlations for mean and envelope orography forecasts are presented for each horizontal resolution in Fig. 8. In winter, the beneficial overall impact of the envelope is evident for all resolutions other than T21. Up to day 4 there is a gradual change from T21 to T106, with a clearly damaging effect of the envelope at T21, a slight worsening at T42, and improvements at T63 and T106, these being noticeable earlier in the forecast range for T106. Later in the forecast range, quantitative aspects of the improvement due to the envelope at resolutions higher than T21 must be regarded with caution because of sampling uncertainties; one case at T42 contributes more than 2% to the mean difference

for day 10, and the improvement at T63 and T106 from the six cases for winter 83/84 was substantially larger than from the corresponding cases for 84/85. On average the T63 improvement is somewhat smaller than the one reported in Wallace et al. (loc.cit.).

The results for summer shown also in Fig. 8 are in sharp contrast. The envelope has a detrimental effect across the whole forecast range for T42 and T63, and only for T106 resolution is the performance of the mean and envelope orographies comparable. When results are averaged over the whole 24 cases, the envelope is clearly detrimental at T21 and beneficial at T106. Over the full range of annual conditions, the evidence in favour of the envelope is at best marginal for T42 and T63. Fig. 8 also indicates that for T106 there is little to choose, overall, between one and $\sqrt{2}$ standard-deviation envelopes, the higher orography giving slightly better results in winter, and slightly poorer results in summer.

Scatter diagrams showing individual forecast comparisons between mean and ($\sqrt{2}$) envelope orographies for all resolutions for day 4, and for T63 and T106 for day 7 are presented in Fig. 9. For T21, there is considerable dispersion along the diagonal, indicating a highly variable forecast quality, with particularly poor results in summer cases (denoted by + signs). Accuracy is considerably higher for the other resolutions at day 4, and it can be seen that there is less scatter across the diagonal for T63 than for T42, and less still for T106, indicating (as might be expected) a decrease in sensitivity to the envelope as resolution increases. There is nevertheless a larger mean improvement due to the envelope at T106 because the small differences are more systematically in favour of the envelope. There is more variability at day 7, and seasonal differences are more clear, particularly at T63 for which the improvement due to the envelope in winter and deterioration in summer occur in almost all cases. Examining other levels and variables generally confirms these results, but suggests a slightly more positive impact of the envelope at T63, and a more systematic benefit at T106, for the 500 mb temperature and 850 mb wind fields. A similar response is obsersved for the 1000 mb and 500 mb height fields.

6.3 Synoptic assessment for the Northern Hemisphere

A detailed synoptic assessment of forecasts has been carried out, concentrating on the evolution of forecast differences from what are typically, in

the early part of the 10-day range, small deviations localized in particular mountainous regions. Earlier reports have emphasized the importance of the Rocky Mountain chain; here we illustrate how several other mountain ranges prove to be important in turn or simultaneously.

Fig. 10 displays day 7 forecasts of 500 mb height and difference maps for the January 1984 case for T106 and mean and ($\sqrt{2}$) envelope orographies. Differences are particularly large over the Bering Strait and North Asia in connection with a different position of a strong anticyclone. In the analysis and envelope-orography forecast the anticyclone is positioned at 150°E and a ridge extends southwestwards towards Siberia. With the mean orography the anticyclone is displaced by more than 20° eastwards and a low pressure belt has broken the associated ridge. By looking backwards in time, it was possible to trace the origin of these (slowly moving) differences to the mountains of East Asia. Also evident in Fig. 10 are differences over Western Europe and the North Atlantic, again in favour of the envelope. These can be traced back to northeastern North America and the south of Greenland. Fig. 10 also includes a plot of differences between the two envelopes tested at T106 resolution; in this case the patterns of difference are similar to those between envelope and mean, and amplitudes are also in approximate proportion to the difference in orography. It must be stressed that this is not generally the case, as found in the following example.

A crucial role of an envelope in the formation of a European block is shown in Fig. 11, which displays 7-day forecasts from 15 March, 1984 with T106. Differences are particularly large over Northwestern Europe and the North Atlantic, and the structure of the block is well captured with the envelope but not with the mean orography. Here, the result from the one standard deviation envelope is shown, but in this case a very similar forecast was obtained using the $\sqrt{2}$ envelope. Five-day mean maps for the one standard deviation envelope have been shown already in Fig. 2, and the corresponding $\sqrt{2}$ envelope map is included later in Fig. 18.

In summer, the deterioration observed at T63 resolution due to use of the envelope appears over several areas. On a number of occasions it is quite large over the North Atlantic and Europe, on other occasions over the North

Pacific, but rarely over North America. This appears to be a consequence of a lesser role of the Rocky Mountains in summer, when the main flow is located in a more northerly position.

One of the critical areas for the interaction between the flow and the orography is Greenland and the mountainous islands to the west. In five of the twelve cases, and in others outside this sample, large differences over the North Atlantic, Europe and North Asia appeared to originate from this region, leading in most cases to a degradation of forecasts when using an envelope.

A clear example is shown in Fig. 12, which presents day 4 forecasts from 15 May 1984 by T63 and T106. At T63 there is a large (although small-scale) difference over the North Atlantic associated with a cut-off low south of Iceland, which later results in a very different forecast over Europe, albeit by then at a time range when neither mean nor envelope forecast is very good. Examination of the evolution in time of difference maps shows how this difference developed from the area west of Greenland, where the flow was active in this situation. Other differences can be seen in the position of the cut-off over Spain and the intensity of the ridge over the Rocky Mountains both differences having grown in situ. Over North Asia a low is further south when using the mean orography, as has been observed on several other occasions.

Fig. 12 also shows how differences between mean and envelope forecasts are generally smaller for T106, particularly over the North Atlantic. This is likely to be due to a better definition of the fairly high but isolated mountains west of Greenland; at T63 these appear as a broad mountainous extension of Greenland, particularly in the case of the envelope orography.

An example of large differences over eastern Siberia and the North Pacific is shown in Fig. 13. This presents 6-day forecasts from 15 June 1984. The envelope-orography forecast exhibits major phase errors with respect to the deep cut-off low off the Asian coast and the trough near 150°W, these errors being substantially less for the mean orography. Here, as in several other cases, differences could be traced back to the Siberian mountains to the north of the Tibetan plateau. As often in summer, mean and envelope produced more similar forecasts at T106, shown also in Fig. 13.

Detrimental effects of an envelope representation of the Asian mountain ranges is sufficiently widespread to be evident in regional objective verifications. Indeed, while results for many regions are in agreement with the Northern Hemisphere figures presented previously, anomaly correlations computed for a region including much of China and Japan reveal generally poorer results, even in winter, with the envelope orography. Fig. 14 shows this effect to decrease with increasing resolution. A further interesting synoptic example, not illustrated here, occurred in the April, 1984 case. The envelope forecast exhibited an erroneously deep and eastward-displaced trough near 135°E in a manner representative of a systematic deficiency of the operational forecasts for this month. Better results were obtained with the mean orography, and differences originated near the northeastern border of the Tibetan Plateau and the East Siberian mountains. These results are in agreement with limited-area model studies carried out at ECMWF (Dell'Osso and Chen, 1984). In addition, Sumi and Kanamitsu (1984) note a tendency of the T42 JMA model, despite using smoothed mean orography, to overestimate airflow round, rather than over the Tibetan Plateau, in contrast with the situation for the Rockies.

From the evidence accumulated in this study, the impact of the envelope orography is found in individual forecasts to cause local modifications which may develop in situ, but which commonly amplify and propagate principally on synoptic scales and following the upper-air flow, to influence a moderate sector of the hemisphere over a time-range of about 5 days. It is not clear to what extent these cases support the mechanism proposed by Tibaldi (1985), who argued that improved prediction of planetary scales using envelope orography was a consequence of a weakening of the zonal flow due to the higher orography, this giving improved planetary waves through a different, but essentially linear, response to large-scale orographic forcing. Examining maps of the averages over all the winter cases shows differences early in the forecast range which undoubtedly have a significant planetary-scale component, but which can arise only as the average of local differences, and which appear to be directly related to the Rocky Mountains, Greenland and the mountains of Southern Europe and Asia. These differences first grow largely in place, but drift in the second half of the forecast period, suggesting that some planetary-scale adjustment may be taking place.

6.4 The Southern Hemisphere and Tropics

Results for the Southern Hemisphere and Tropics have been briefly examined, and conclusions are mentioned here. A more extensive diagnosis will be carried out subsequently.

In the Southern Hemisphere the sensitivity to orography is, not surprisingly, less at all model resolutions and seasons than found for the Northern Hemisphere, except possibly for the T21 resolution which appears anomalous in a number of respects. In most individual cases examined to date the main differences originated near the Southern Andes and Drake Passage, although they did not grow to the amplitude found for the Northern Hemisphere. This is clearly seen in mean difference maps which exhibit a relatively simple pattern of upstream and downstream propagation in apparent accord with linear Rossby-wave theory.

In the Tropics a large sensitivity to the envelope has been found in the lower troposphere for some objective scores (anomaly correlations of 1000 mb height, absolute correlations of 850 mb wind) but not for standard-deviation or root-mean square scores. The difference increases mostly in the first two days, and is then more or less uniform. This result is found at all resolutions, and is under further investigation.

Zonal-mean distributions of precipitation show no clearly significant increase due to use of the envelope. Since August 1983 the spectral model has included a modified "horizontal" diffusion of temperature to avoid spurious warming of mountain tops and triggering of convective precipitation, and this, combined with the lower ($\sqrt{2}$) envelope and perhaps the use of the spectral technique, probably accounts for the absence of an increase in tropical precipitation of the type reported by Tibaldi (1985).

6.5 The choice of operational T106 orography

It was clear from the first examination of the results presented in preceding sections that the use of an envelope orography was generally beneficial to the quality of synoptic and larger-scale forecasts at T106 resolution. In this respect, there was little to choose between one and $\sqrt{2}$ standard-deviation envelopes. In order to minimize local problems associated with use of an envelope, the lower orography was chosen for final testing and operational implementation of the high resolution model.

7. RESOLUTION EXPERIMENTS

7.1 Introduction

In this section a comparison between T21, T42, T63 and T106 is presented, with emphasis on differences between T63 and T106. The same type of orography is chosen for the presentation of results for each resolution; this is the $\sqrt{2}$ standard deviation envelope used in the previous operational (T63) model. Differences between the two envelopes tested at T106 have been shown in the preceding section to be generally small.

7.2 Objective verification for the Northern Hemisphere

Fig. 15 displays objective scores for the Northern Hemisphere. The upper plots showing mean anomaly correlations of 500 mb height for the summer and winter seasons indicate a general improvement as resolution increases, and also a tendency for convergence at higher resolutions. This does not imply that forecast differences between T63 and T106 are small throughout the forecast range, but rather that what can be quite large differences later in the range (as shown in Fig. 1) are not systematically in clear favour of the higher resolution. More systematically favourable results at this range may be obtained as other sources of error, particularly in the parameterization and data analysis, are reduced. The improvement in going from T63 to T106 is larger in summer than winter, which can be in part explained by the results already presented concerning the better performance of the envelope orography at T106 in summer. Similar results are obtained at 1000 mb.

Although the objectively measured mean improvements of T106 over T63 are small compared with total mean errors, they are nevertheless larger than the net improvement found to result from the use of envelope rather than mean orography at T106 resolution. They are also significantly larger than those observed when comparing spectral and grid-point models (Girard and Jarraud, 1982). Up to day 5 or 6, the improvements due to resolution increases are almost systematic, as illustrated in the scatter diagrams for day 5 which are shown in Fig. 15b.

7.3 Synoptic assessment for the Northern Hemisphere

Synoptic assessment reveals a number of cases in which a large beneficial impact of increased resolution occurs for a particular feature. Fig. 16 shows day 5 forecasts of 500 mb height over Europe by T63 and T106 from 15 May 1984,

together with the verifying analysis. T106 produces a clearly better forecast of the position of the cut-off low over Spain, as well as a less wrong position for the low to the northwest of Ireland. Associated with the former is a large difference in favour of T106 in precipitation forecasts over Spain and France. The influence of orography in this case was discussed in the preceding section in reference to Fig. 12.

Another example of a large impact of resolution is presented in Fig. 17 for day 3 forecasts by T42, T63 and T106 from 15 September 1984. The analysis for 18 September shows a deep low located just south of Iceland, which over the preceding three days had moved rapidly from its initial position near Florida and amplified substantially. At the 3-day range there is virtually no indication of the low in the T42 forecast, and only a weak feature at T63. T106 on the other hand produces a much stronger development. The low is slightly shifted to the west, but the forecast is altogether much more useful, with a better indication of the associated frontal structure in the 850 mb temperature field.

Although not always as dramatic as the above case, an almost systematic improvement is brought about by use of T106 in situations with rapidly developing lows in the first half of the forecast range. A better definition and position of the associated fronts is particularly evident. Beyond day 5 the situation is less clear, since small-scale lows are much less accurately located, and the prediction of deeper systems by T106 can lead to worse objective scores. This was found to be the case in detailed synoptic assessment of the two cases (out of the first 18) exhibiting the poorest objectively-measured performance of T106 relative to T63.

As already mentioned, the beneficial impact of higher resolution is on average smaller in winter, at least according to objective verification. Major sensitivity is nevertheless found on a number of occasions. A pronounced example, which has already been referred to, is shown in Fig. 18 by means of 5-day mean maps of 500 mb height for days 5 to 10. The structure of the block over the northern regions of the Atlantic and Europe, which has already been shown to be sensitive to orography, is clearly better at T106 than T63, and the T42 forecast is poorer than either. The downstream ridge over western Asia is also captured better at T106. Fig. 1 in fact shows that in this

extreme case, the T106 forecast (with one standard-deviation envelope) at day 10 is closer to reality at 500 mb than it is to the T63 forecast.

As suggested by the scatter diagrams for the China/Japan region which are included in Fig. 15b, forecasts over East Asia proved to be particularly sensitive to resolution, and in most cases improved distinctly when using T106. An example of such a difference is shown in Fig. 19. The trough extending towards Japan is forecast by T63 to be too deep, and displaced too far to the east, contributing to a systematic deficiency noted earlier for the month in question, April 1984. Both errors are reduced by T106. Elsewhere, however, in stark contrast to the case discussed in the preceding paragraph, T63 and T106 are in general agreement, and very inaccurate. The erroneous cut-off low near 180°E is much more pronounced at T106.

Small improvements in synoptic-scale forecasts coupled with a finer orographic description can combine to yield pronounced improvements in precipitation patterns as resolution increases. Illustrated in Fig. 20 is precipitation accumulated between days 2 and 3 of T63 and T106 forecasts from 15 September 1983, together with corresponding observed values, observations of no rain being denoted by a dot. T63 produces only one zone of heavy rain centred over Hungary and extending well over Austria, Yugoslavia and Poland. T106 on the other hand forms two main centres of heavier rain, and a less widespread distribution, in good agreement with the observations. Both forecasts failed to predict the showery rainfall observed over Italy. Other experimentation has shown that in regard to precipitation, the two resolutions respond in a generally similar way to changes in the parameterization of moist processes.

Maps of the mean error of 500 mb height averaged for days 8-10 of the forecast range and for the 12 "winter" cases are shown in Fig. 21. The errors at T21 resolution bear some similarity in pattern to those at higher resolution, but the predominant difference is between T21 and T42 rather than between T42 and higher resolutions. The hemispheric root mean square of this mean error is also rather higher at T21 than at other resolutions, in contrast to results showing a deterioration with increasing resolution in climate simulations of the Northern Hemisphere height field (Manabe et al., 1979, Cubasch, 1981). Differences between T42 and higher resolutions vary from location to location, and the sample size may not be sufficient to assign significance to most of

these. However, there is no suggestion of an overall worsening of mean forecast errors with an increase in resolution from T63 to T106. Earlier in the forecast range, mean errors generally decrease with increasing resolution.

Close inspection of Fig. 21 reveals that tropical height biases are very similar at T42 and T63, but are substantially smaller at T106. Overall, T106 yields a fall of 0.7 K in the erroneous global-mean cooling. This cooling is very similar at T42 and T63 and experiments suggest that the experiment at T106 can be largely accounted for by the reduction in horizontal diffusion, particularly on the divergence field. Seven of the twelve cases included in this sample were carried out with the former operational parameterization schemes, for which the reduced cooling with T106 is clearly beneficial. With the new parameterization schemes, which were developed at T63 resolution, T106 tends to enhance a small general warming of the middle troposphere.

7.4 The Southern Hemisphere and Tropics

In the Southern Hemisphere the mean impact of resolution on the objective verification of forecasts is small for resolutions above T42, as can be seen in the scatter diagrams presented in Fig. 22. The spread across the diagonals is somewhat smaller than shown in Fig. 15 for the Northern Hemisphere, indicating a smaller sensitivity to resolution, but the main difference is that improvements due to resolution are largely systematic up to day 5 in the Northern Hemisphere, whereas resolution differences above T42 do not lead to systematic improvements in the other hemisphere. Further diagnosis is required to identify reasons for this. Mean 500 mb height errors show little variation between T42, T63 and T106, but are very substantially larger for T21, which significantly underestimates the strength of the westerly mid-latitude flow, this being in agreement with results from the climate simulations referred to previously.

In tropical and subtropical regions some sensitivity has been found in the prediction of cyclones or intense depressions. If present in the initial data, these systems are slightly deeper in T106 forecasts and tend to follow somewhat more accurate tracks. Another significant difference has been found in the prediction of the mid-tropospheric temperature field over South Asia, as shown by the objective verification included in Fig. 22, but no synoptic interpretation has been sought to date.

8.4 Impact of the revised model on data assimilation

It was also noted in section 2 that extensive testing of the impact of the resolution increase on data assimilation could not be carried out. However, results are available showing the net impact of the resolution increase and parameterization change during the quasi-operational trial of the revised model.

In general, differences between the operational and test analyses were small. The comparisons of first guesses with observed winds and heights revealed smaller root-mean square differences for the test assimilations, with a reduction in wind differences from 5.2 to 5 m s^{-1} at the tropopause. Occasional differences in data acceptance were generally considered to be in favour of the trial system, which tended to yield mid-oceanic surface lows deeper by a millibar or two. A more pronounced, and expected, impact on the tropical humidity fields was almost certainly associated with the new treatments of convection.

Definitive measures of the impact of the analysis differences on forecast quality are not available, but a series of forecasts have been carried out for two cases, using the new parameterizations. T63 and T106 forecasts were carried out from the T63 operational analyses, the T106 dataset being produced using the same procedures as for the main experimental programme reported previously. These forecasts were compared with T106 forecasts produced from the trial analyses.

Objective verification of the 500 mb height fields is presented in Fig. 25. Comparing first the T106 forecasts, a slight improvement is seen in the upper plot (for 8 April initial conditions) to result from use of the trial analysis. The converse is the case, and to a larger degree up to day 5, in the lower plot, for 15 April. It can also be seen that T63 provided a better forecast than either T106 prediction from 8 April, and it matches the better of the T106 forecasts from 15 April. In this respect results are at variance with those obtained previously over a wide range of cases, and conclusions as to the sensitivity to analysis differences cannot be generalized.

8.5 Results from the quasi-operational prediction trials

A total of 28 forecasts was carried out during the quasi-operational trial of the high resolution model and new parameterizations. The results were such

as generally to favour the test model, but the impact when measured by objective verification over the Northern Hemisphere was smaller than in the experimentation reported earlier in this paper. The atypicality of two individual cases has already been noted in the discussion of Fig. 25.

A sample of results from objective verification of the full series of trial forecasts is presented in Fig. 26. Mean anomaly correlations computed for the whole Northern Hemisphere indicate a distinct improvement at 1000 mb up to day 5½, but a very marginal one up to this stage at 500 mb, with worse results thereafter at the latter level. A more marked improvement is found over Europe (also shown in Fig. 26a), and over the North Atlantic and Pacific. The scatter diagrams shown for day 4 in Fig. 26b not surprisingly show more spread than found for the resolution increase alone, but a substantial majority of cases is improved at this forecasts range.

The overall assessment of the synoptic character of the differences between trial and operational forecasts is in agreement with that of earlier experiments, and will not be repeated here. Instead, we simply illustrate in Fig. 27 the day 4 forecasts of sea-level pressure and 850 mb wind, and verifying (operational) analyses, for the case which height anomaly correlations computed for Europe and the Mediterranean indicate is the most sensitive to the change in model. The test forecast is obviously better in its treatment of the major anticyclone and the low east of Iceland, and less obviously better in prediction of the Mediterranean low. Improvements show up clearly in the 850 mb wind over the United Kingdom, the North Sea and much of Scandinavia, and improvements in detail over Italy can be seen in this field.

9. CONCLUDING REMARKS

Few major problems have been encountered in the preparation of the high resolution model for operational prediction. Practical difficulties during technical development proved surmountable, the ideas for time-step enhancement worked surprisingly well, and effective solutions were found for problems associated with boundary-layer stability and surface fields. The choice of envelope orography at T106 resolution was clear cut, and some distinct improvements in forecast quality in changing from T63 to T106 resolution have been revealed by the experimental programme.

The ancillary experimentation involving lower resolutions and mean and envelope orographies has proved useful in placing the change from T63 to T106 in context, and in understanding the previous operational performance of the T63 model with envelope orography. The very poor results obtained with T21 rule it out as a tool for much research use at ECMWF, but it is clear from, for example, the similar mean error patterns of 500 mb height found for other resolutions that much future development and testing can be carried out at T42 and T63 resolutions. Despite this, some appreciable differences between T63 and T106 have been found in mean temperature biases and in tropical precipitation maps.

The marked seasonal sensitivity of Northern Hemisphere forecasts to the choice of mean or envelope orography is of interest. The detrimental effect of the envelope in summer found at resolutions lower than T106 appears from synoptic assessment to follow from interactions between the flow and mountain ranges which are relatively less important in winter due to the more southerly location of the main jet. What is less clear at present is the extent to which this is a consequence of a general poor representation of these particular ranges by the envelope approach, or of the envelope being generally less appropriate in summer than winter. Quite apart from such questions, it is expected that the sample of cases examined in some detail as part of this study will serve as useful benchmarks for the evaluation of proposed alternative orographic representations.

The extensive quasi-operational trial of the high resolution model and new parameterizations yielded a number of improvements in forecast quality, but the overall performance of the revised model relative to the operational T63 model was poorer than previous experiments had suggested would be the case.

Tests such as have been presented in Fig. 25 suggest that there were no unexpected problems in the previously untried combination of increased resolution, new parameterizations, revised surface fields and data assimilation. Rather, it is likely that the prevailing, fairly persistent, synoptic situation during the period of the trial was such as to give atypical results.

Operational experience with the revised model is encouraging. Synoptic-scale forecasts have been assessed both subjectively and objectively as generally better than found previously for this time of year, although interannual variability prevents quantification of the improvement. Some biases in precipitation and surface temperature have become more pronounced, but have been at least partially reduced by recent adjustments of the parameterization of evaporation and convection. Detailed feedback from the Member States' forecasters has yet to be received, and it will be only with this, and the general objective assessment over the coming year and more, that a full picture of the performance of the revised model will emerge.

References

Cubasch, U. 1981: The performance of the ECMWF model in 50 day integrations. ECMWF Tech. Memo. No. 32, 74pp.

Dell'Osso, L. and S-J. Chen 1984: Genesis of a vortex and shear line over Qinghai-Tibet Plateau - numerical experiments. paper presented at the International Symposium on the Tibet Plateau and mountain meteorology. March 1984, Beijing, China.

Girard, C. and M. Jarraud 1982: Short and medium range forecast differences between a spectral and a grid point model. An extensive quasi-operational comparison. ECMWF Tech.Rep. No. 32, 178 pp.

Manabe, S., D.G. Hanu, J.L. Holloway 1979: Climate simulation with GFDL spectral models of the atmosphere: effect of spectral truncation. GARP publication, Series No.33, 41-94. WMO, Geneva, Switzerland.

Simmons, A.J. and M. Jarraud 1984: The design and performance of the new ECMWF model. Proceedings of the 1983 ECMWF seminar.

Sumi, A. and M. Kanamitsu 1984: A study of systematic errors in a Numerical Weather Prediction model. Part I: General aspects of the systematic errors and their relation with the transient eddies. J.Met.Soc. Japan, 62, 234-251.

Tibaldi, S. 1985: Envelope orography and maintenance of quasi-stationary waves in the ECMWF model. To appear in Advances in Geophysics.

Volmer, J.P., M. Déqué and M. Jarraud 1983: Large scale fluctuations in a long range integration of the ECMWF spectral model. Tellus, 35A, 173-188.

Wallace, J.M., S. Tibaldi, A.J. Simmons 1983 Reduction of the systematic forecast errors in the ECMWF model through the introduction of an envelope orography. Quart.J.Roy.Met.Soc., 109, 683-717.

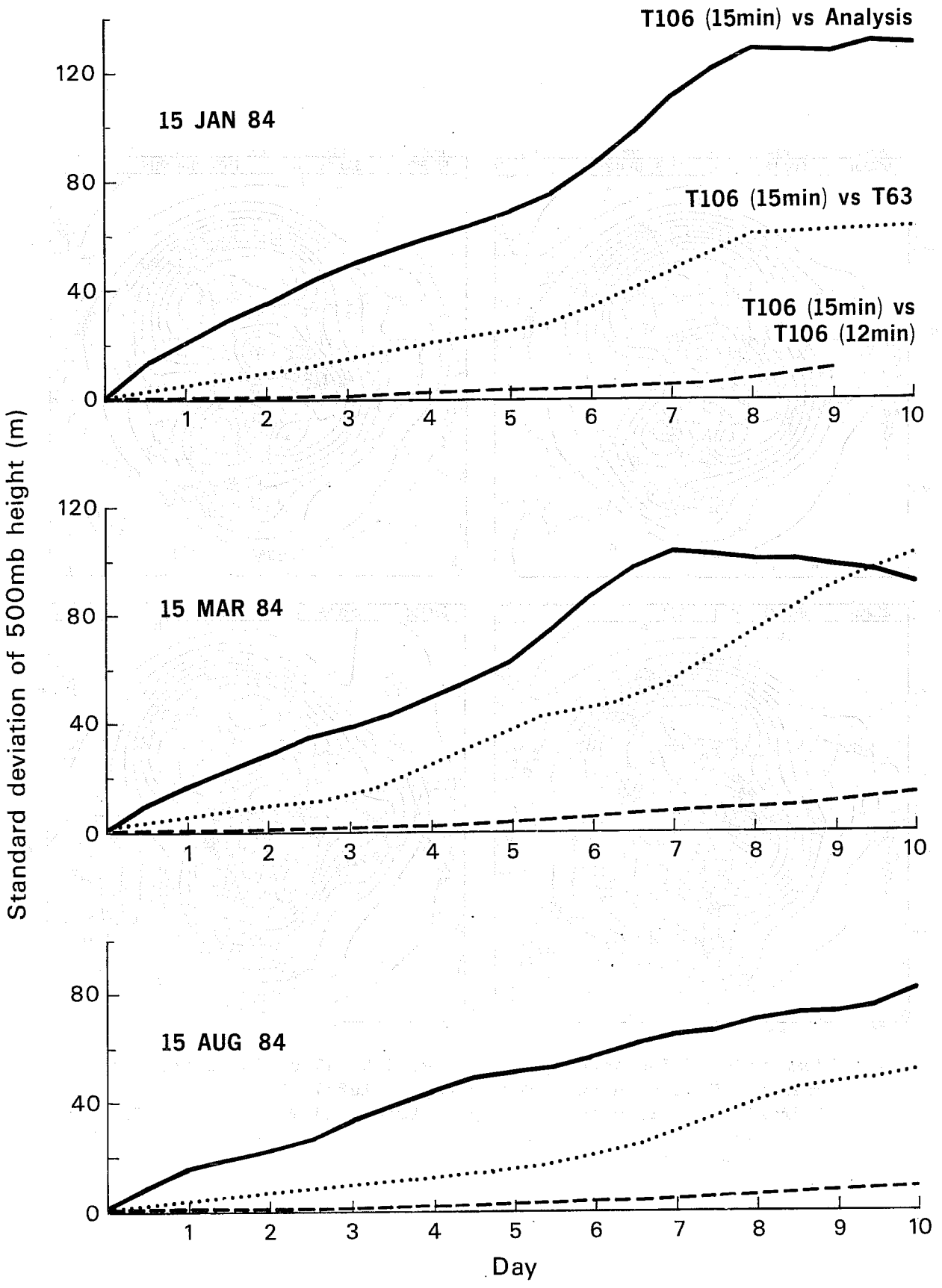

Fig. 1 Standard deviations of 500 mb height (m)computed over the extratropical Northern Hemisphere for 3 cases, with T106 forecasts with modified diffusion and 15 minute timesteps compared with

Solid line : Analyses
Dotted line : T63 forecasts
Dashed line : Standard T106 forecasts with 12 minute timesteps

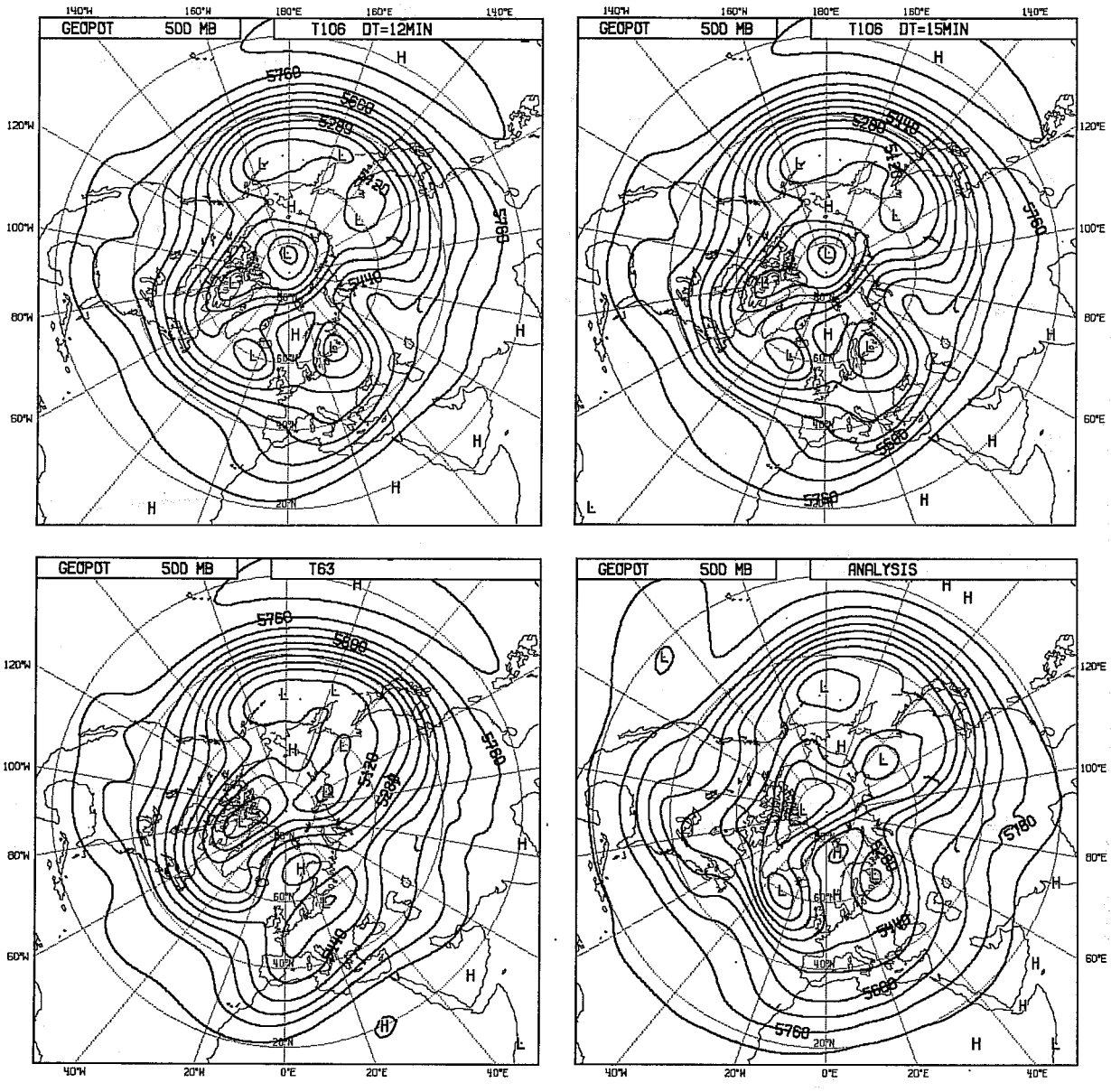

Fig. 2 Mean maps of 500 mb height for days 5 to 10 of forecasts from a standard T106 with Δt = 12 min (upper left), T106 with modified diffusion and Δt = 15 min (upper right) and T63 (lower left). The verifying mean analysis is shown in the lower right panel. The initial date of the forecasts was 15 March 1984.

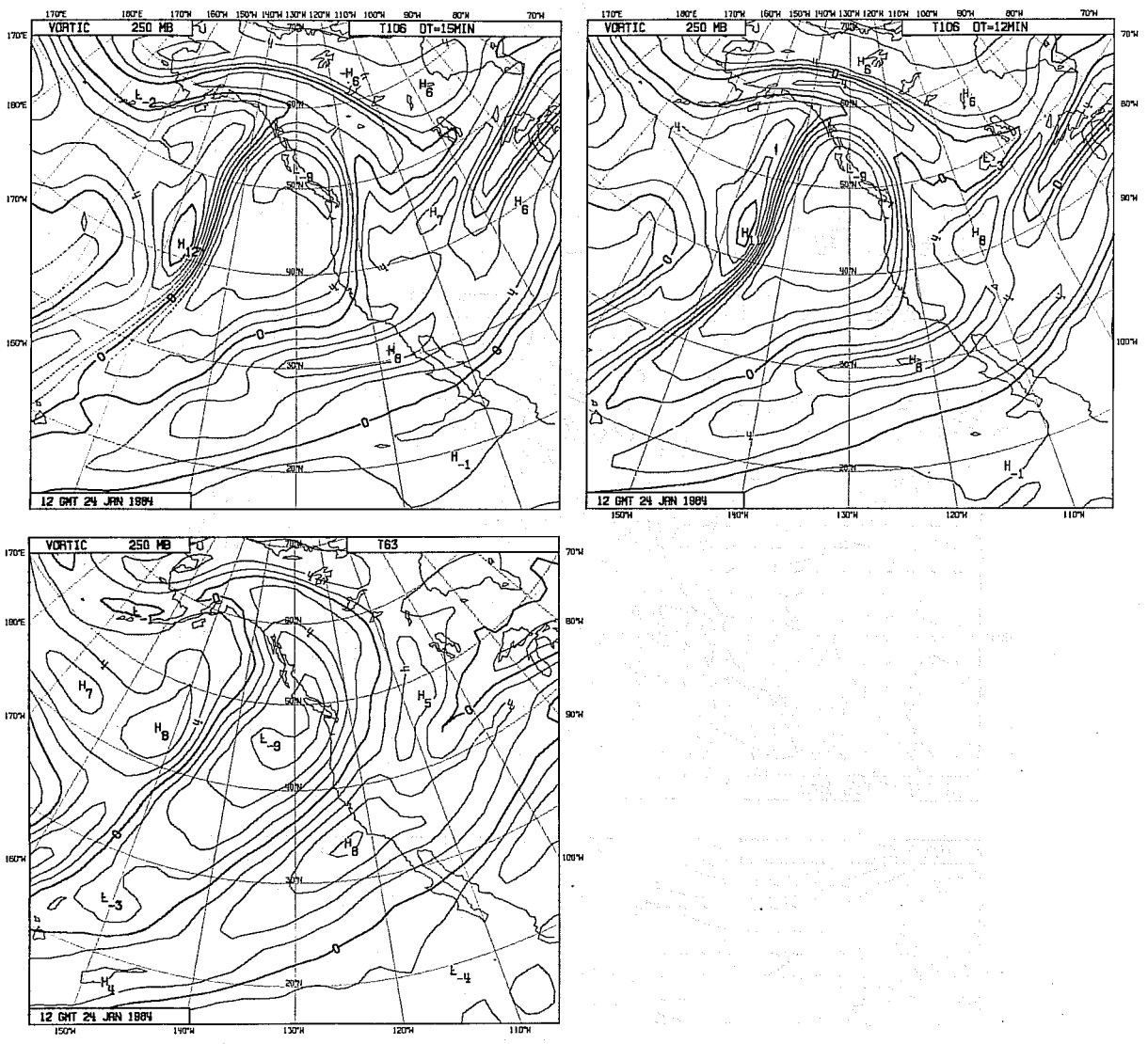

Fig. 3 Maps of relative vorticity (in units of 10^{-5} s^{-1}) at 250 mb for D+9 forecasts from 15 January 1984. T106 forecasts with 12 and 15 minute timesteps are shown in the upper right and left hand plots respectively, and the T63 forecast is shown in the lower plot.

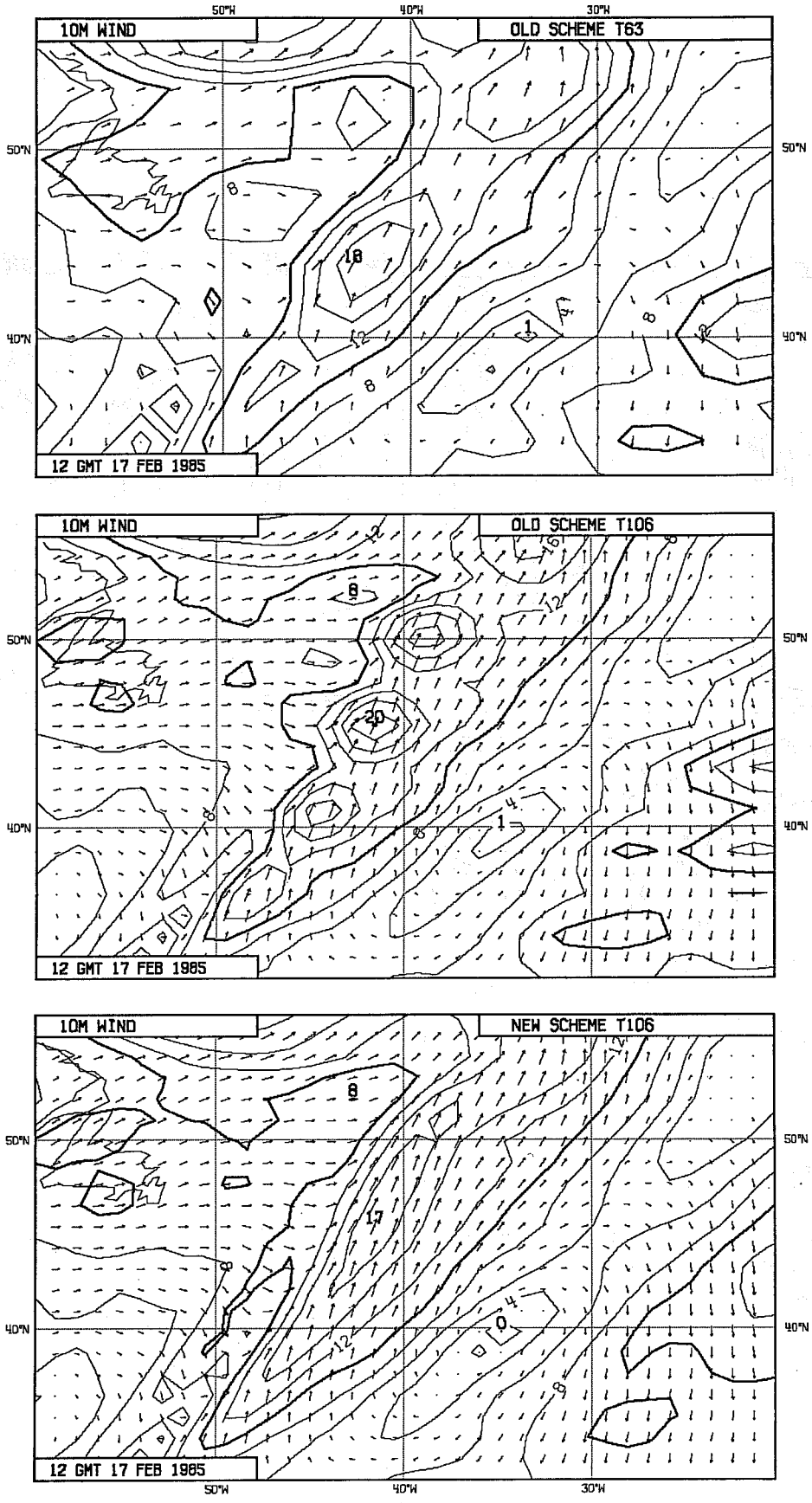

Fig. 4 D+2 forecasts of 10 m wind over the North Atlantic using the former operational time scheme for vertical diffusion at resolutionh T63 (upper) and T106 (middle). The corresponding T106 forecast with the modified time scheme is shown in the lower map. The contour interval is 2 m s^{-1}.

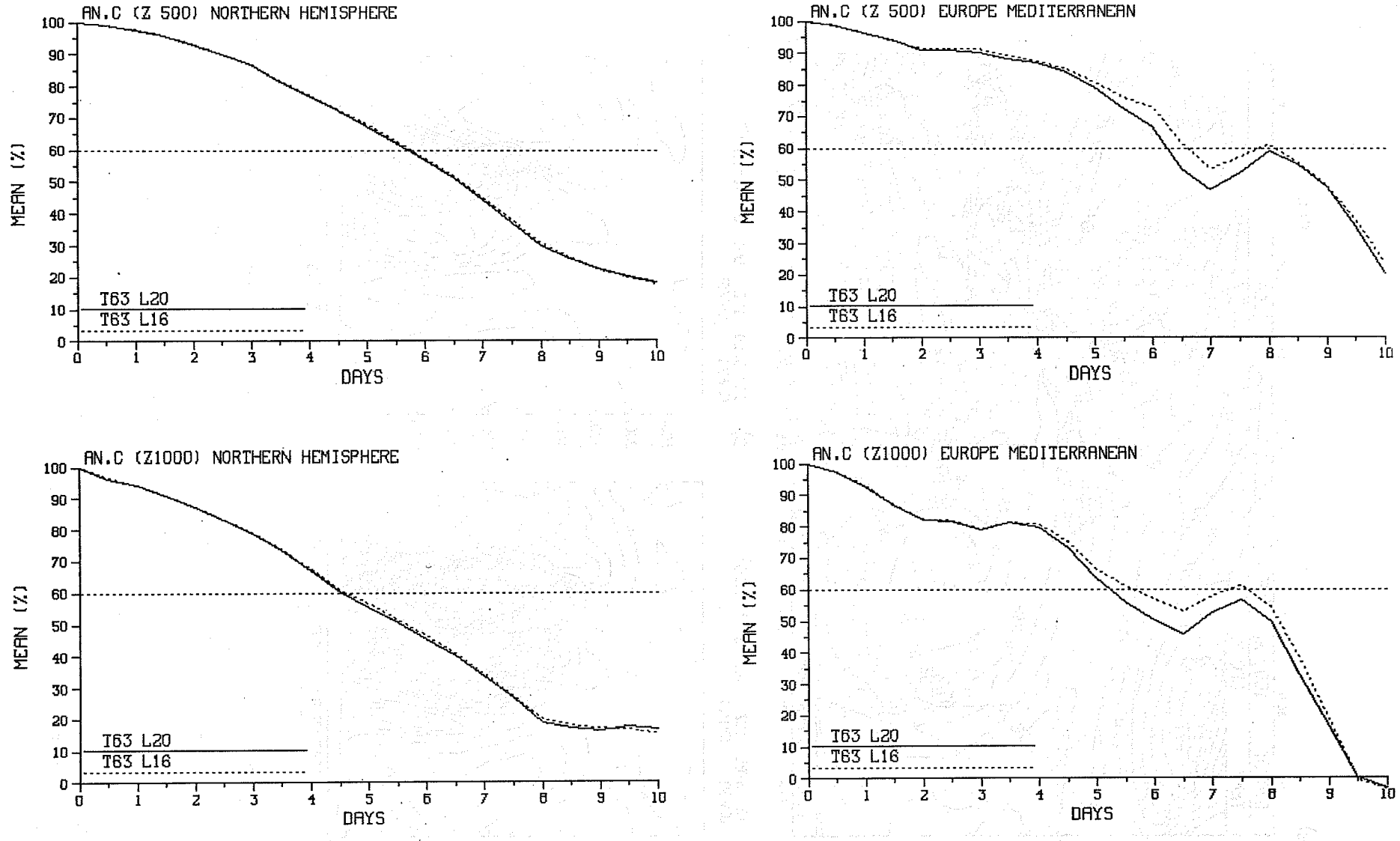

Fig. 5 Mean anomaly correlation of height at 500 mb (upper) and 1000 mb (lower) averaged over 8 cases for the Northern Hemisphere (left) and Europe (right). Full lines correspond to T63 with 20 levels and dotted lines to T63 with 16 levels.

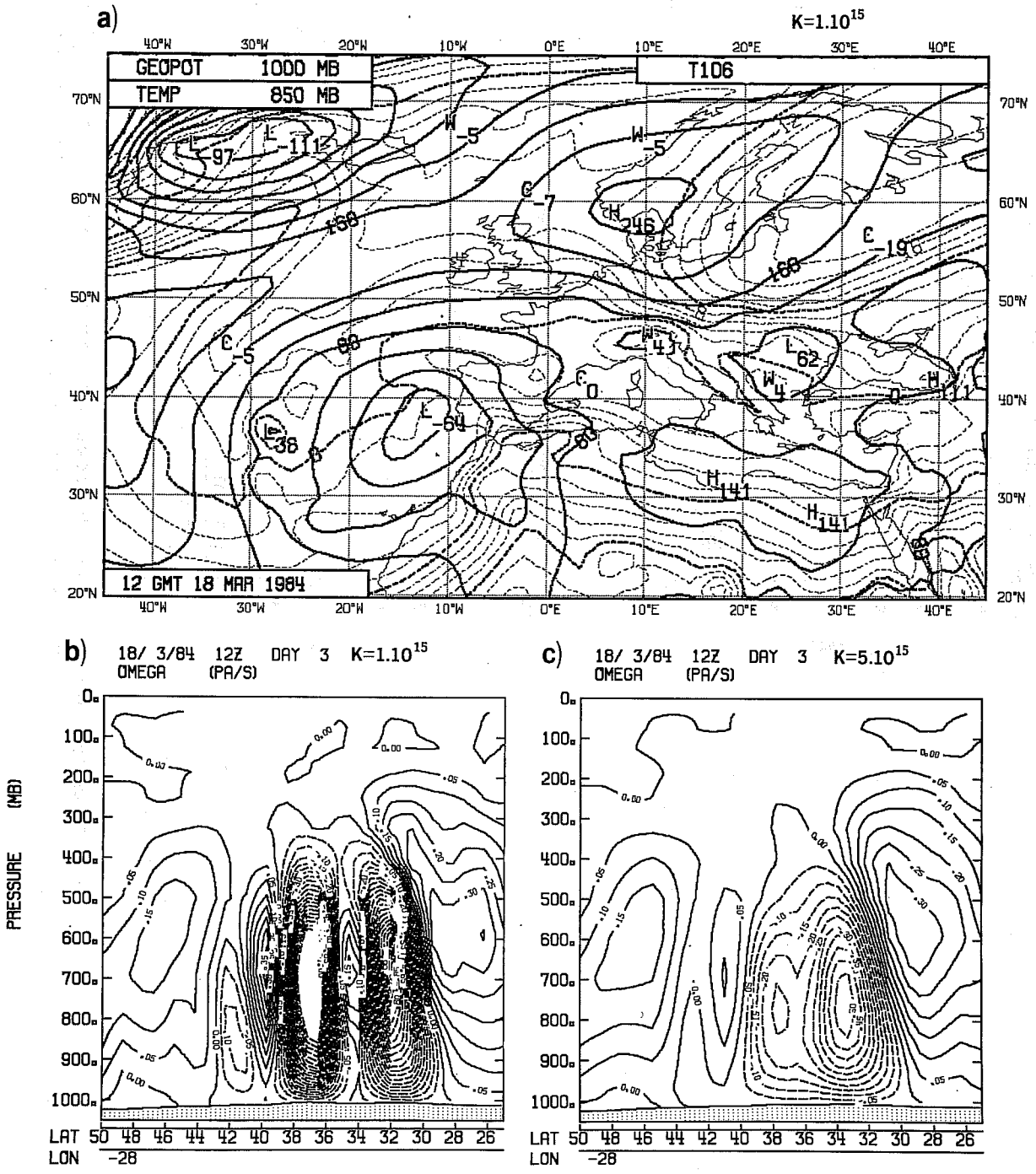

Fig. 6 (a) D+3 T106 forecast of 1000 mb height and 850 mb temperature fields (15 March 1984 case) using a low diffusion coefficient for divergence ($K=1.10^{15}$ m^4 s^{-1})

(b) Corresponding cross section of vertical velocity at 28°W and from 26° to 30°B.

(c) As (b) but using a stronger diffusion coefficient for divergence ($K=5.10^{15}$ m^4 s^{-1}).

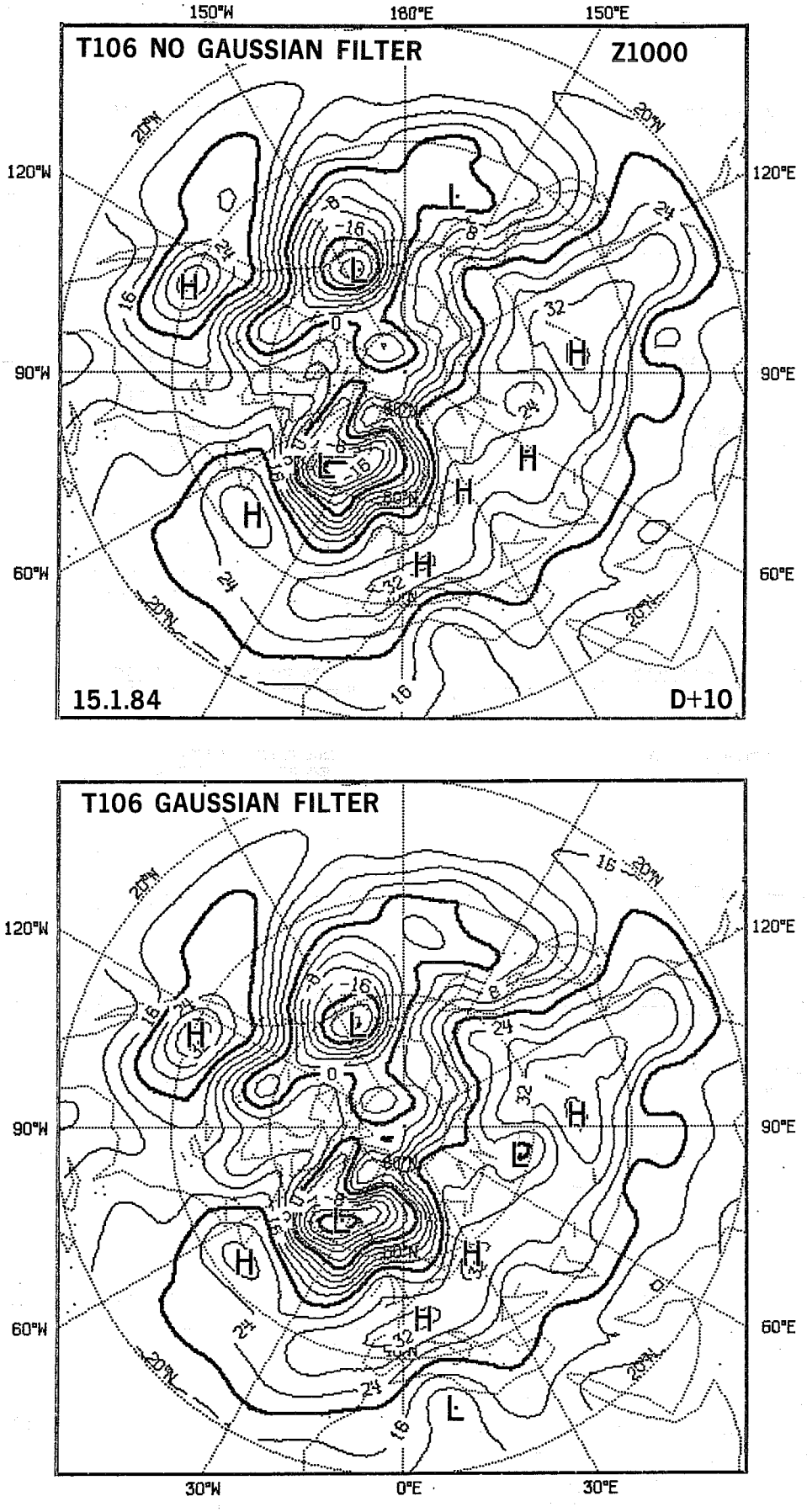

Fig. 7 D+10 T106 forecast of 1000 mb height field (15 January 1984 case) using a ($\sqrt{2}\sigma$) envelope without any Gaussian filtering (upper) and with a weak (50 km radius) filtering (lower).

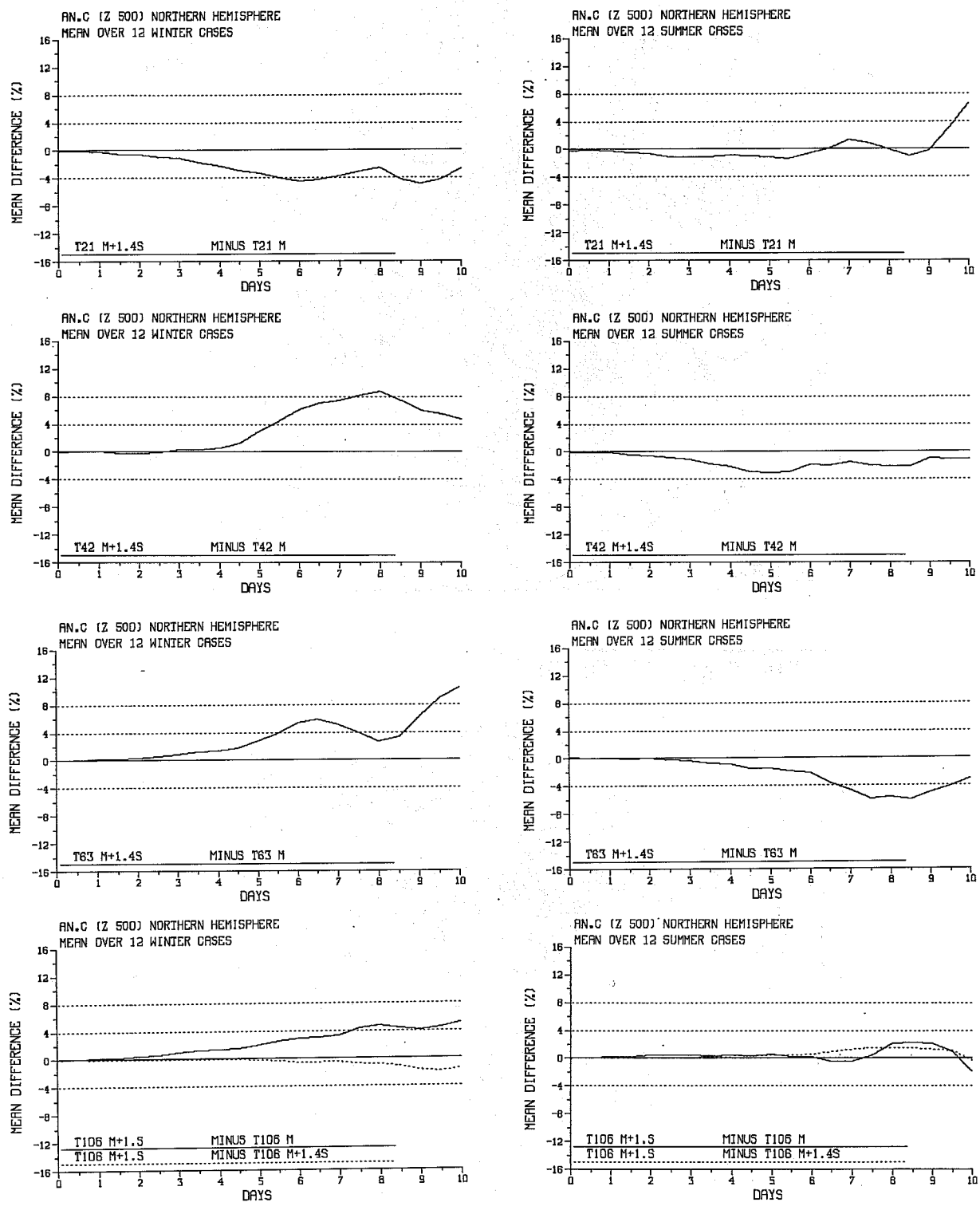

Fig. 8 Mean differences of anomaly correlations of 500 mb height in the Northern Hemisphere between mean and ($\sqrt{2}\sigma$) envelope orographies for T21 to T106 resolutions (top to bottom) averaged over 12 winter (left) and 12 summer (right) cases.
In addition, for T106, the dotted lines correspond to differences between a (1σ) and a ($\sqrt{2}\sigma$) envelope.

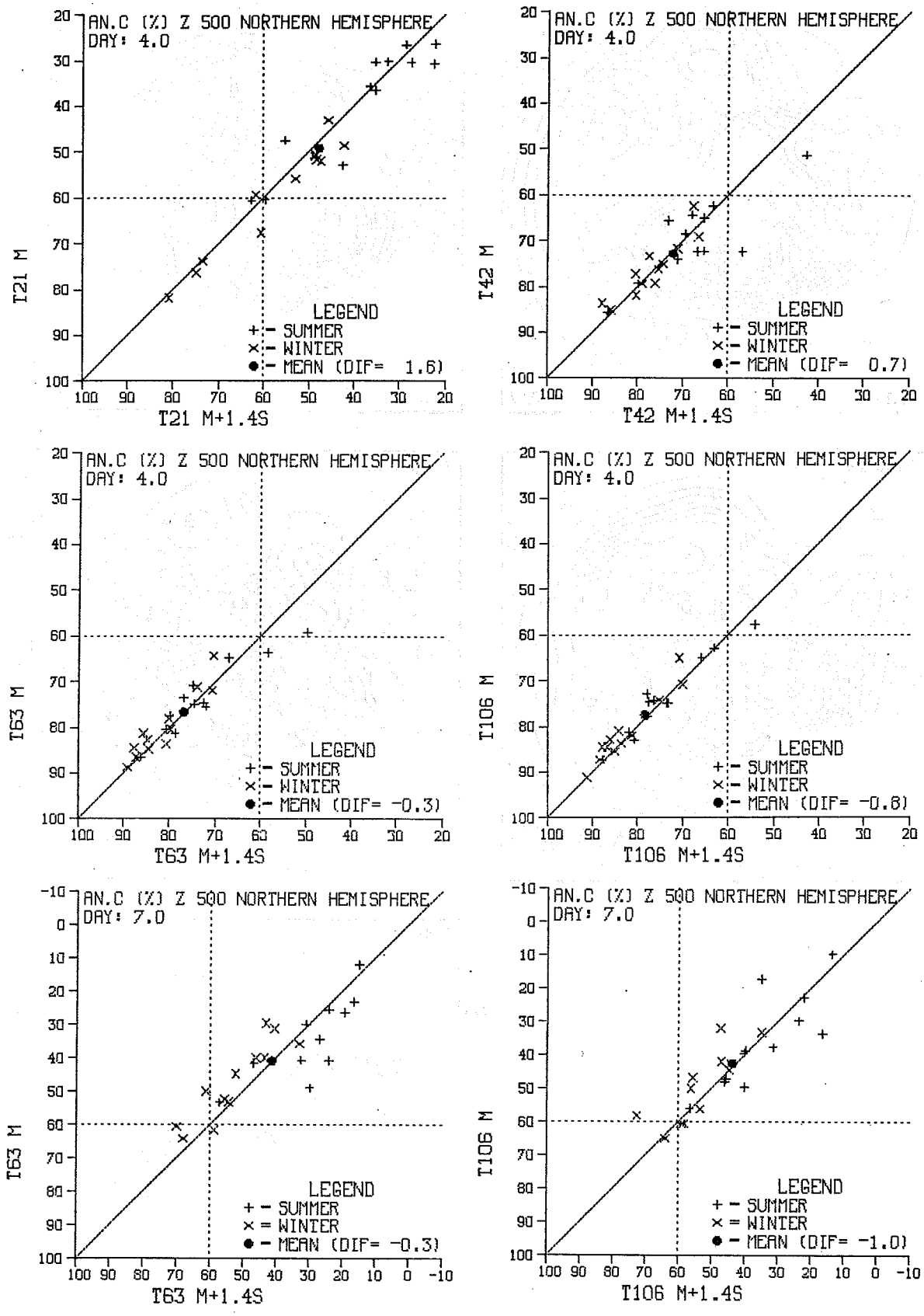

Fig. 9 Upper and middle: scatter diagrams of anomaly correlations of 500 mb height field in the Northern Hemisphere comparing mean and ($\sqrt{2}\sigma$) envelopes at T21, T42, T63 and T106 resolutions for D+4 forecasts.
Summer cases are represented by + signs, winter cases by x signs, and the mean by a thick dot.
Lower: As top for D+7 forecasts at T63 and T106 resolutions.

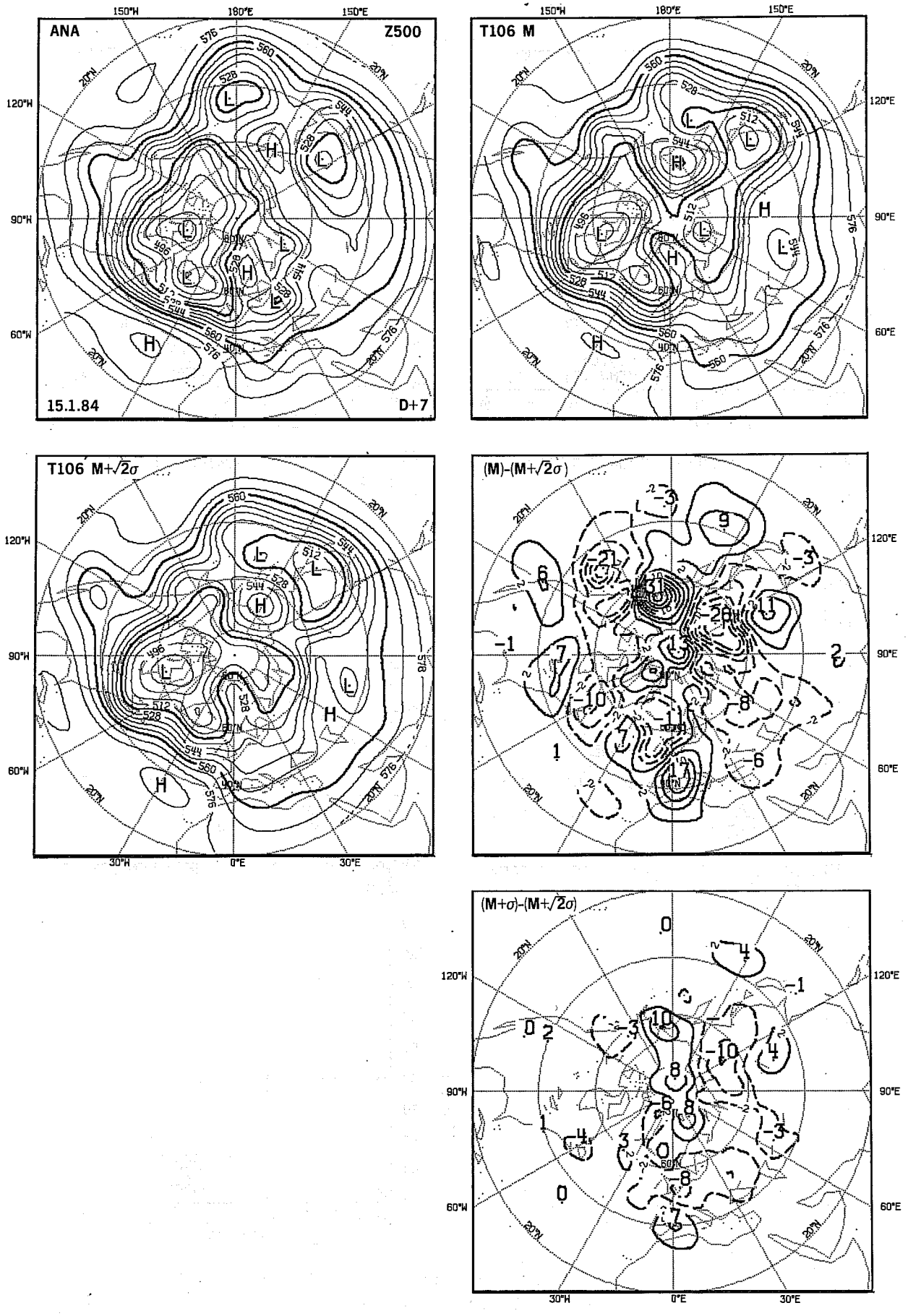

Fig. 10 Analysed 500 mb height field for 22 January 1984 and corresponding D+7 T106 forecasts using a mean and ($\sqrt{2}\sigma$) envelope orography, together with the associated difference map. The map of differences between a(1σ) and a ($\sqrt{2}\sigma$) envelope is displayed at the bottom.

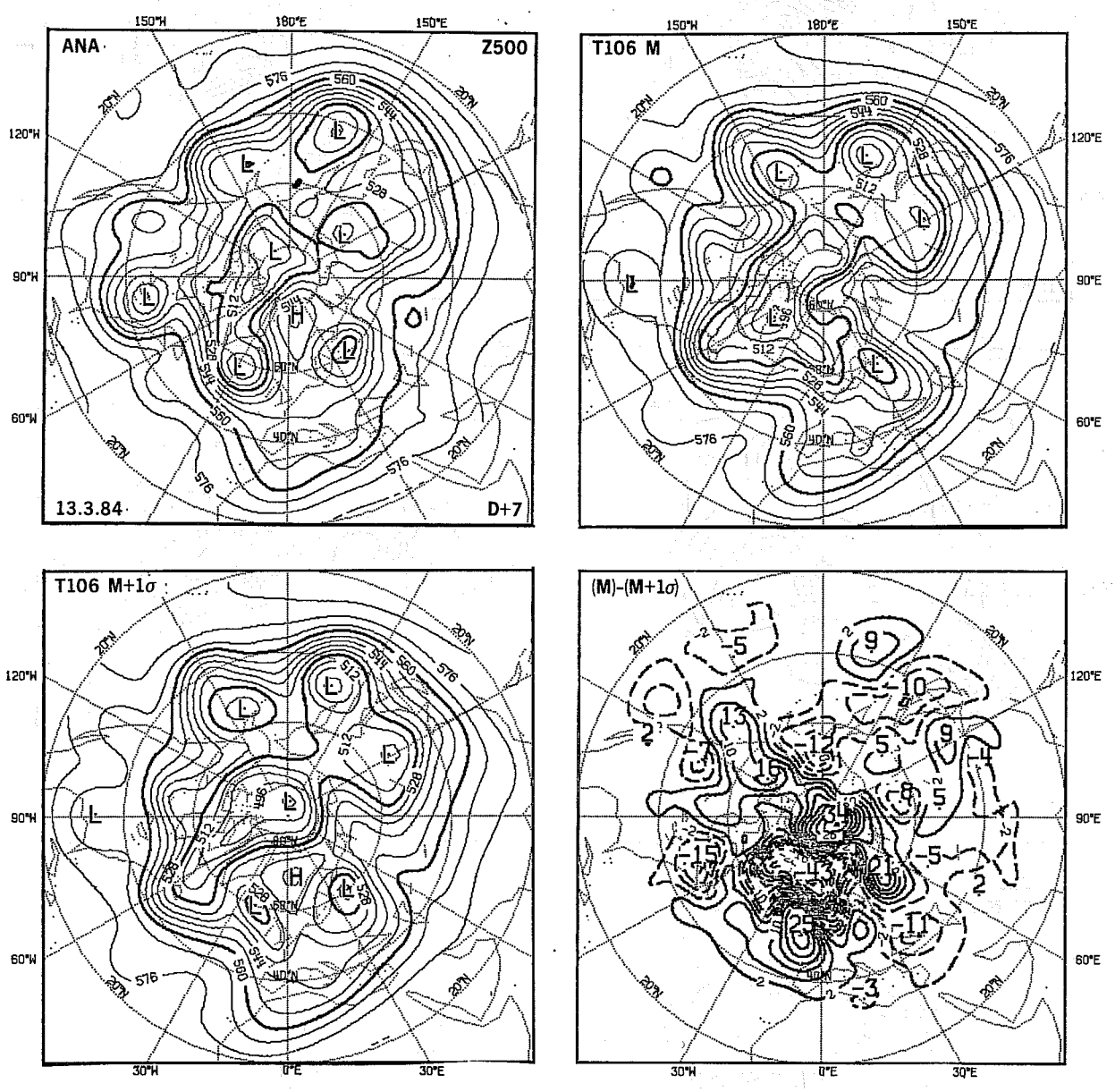

Fig.11 Analysed 500 mb height field for 22 March 1984 and corresponding D+7 T106 forecasts using a mean and a (1σ) envelope orography, together with the associated difference map.

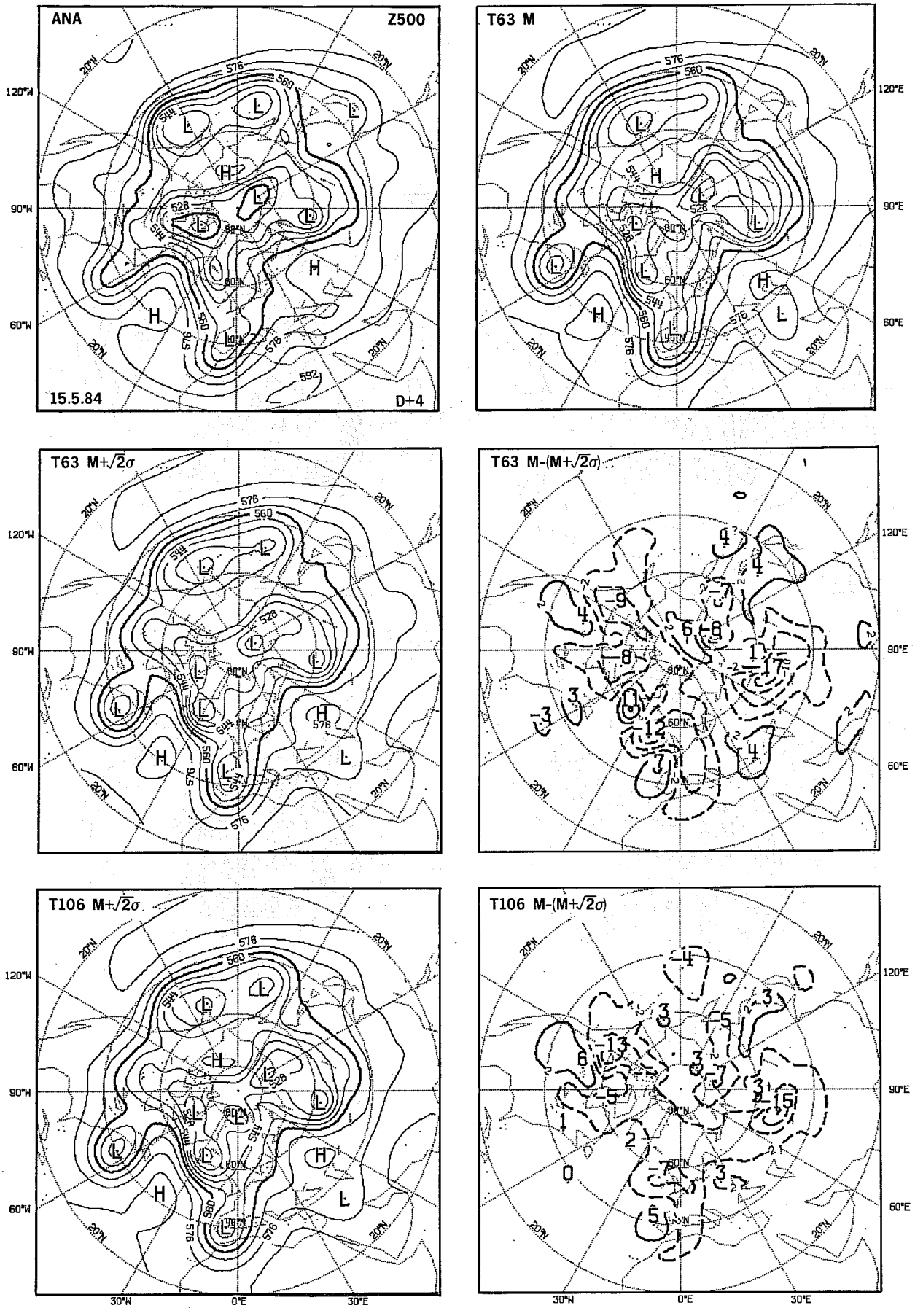

Fig. 12 Upper and middle: Analysed 500 mb height field for 19 May 1984 and corresponding D+4 T63 forecasts using a mean and a ($\sqrt{2}\sigma$) envelope orography together with the associated difference map.
Lower: D+4 T106 forecast using a ($\sqrt{2}\sigma$) envelope and corresponding difference map.

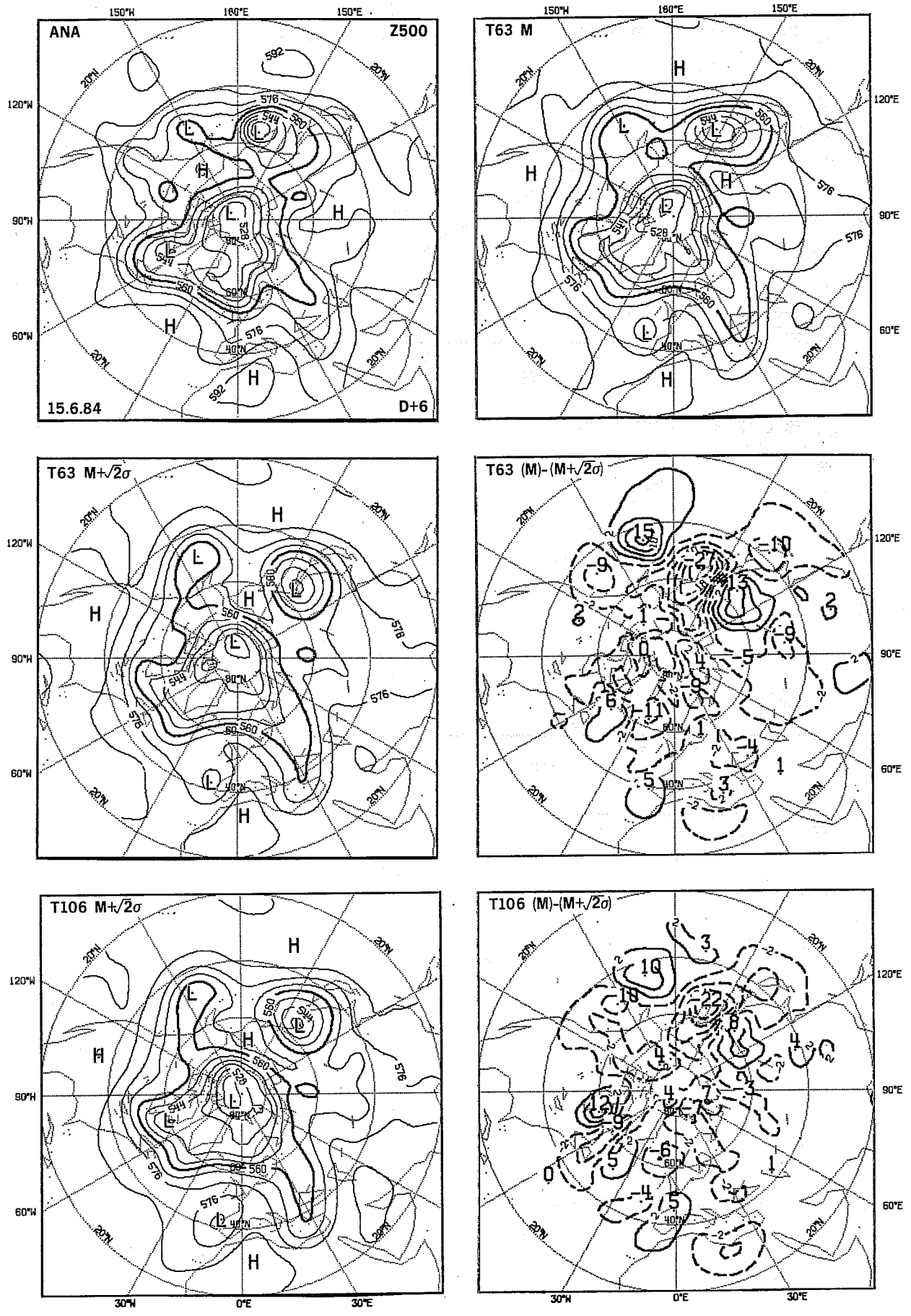

Fig.13 As Fig.12 for D+6 forecasts from 13 June 1984.

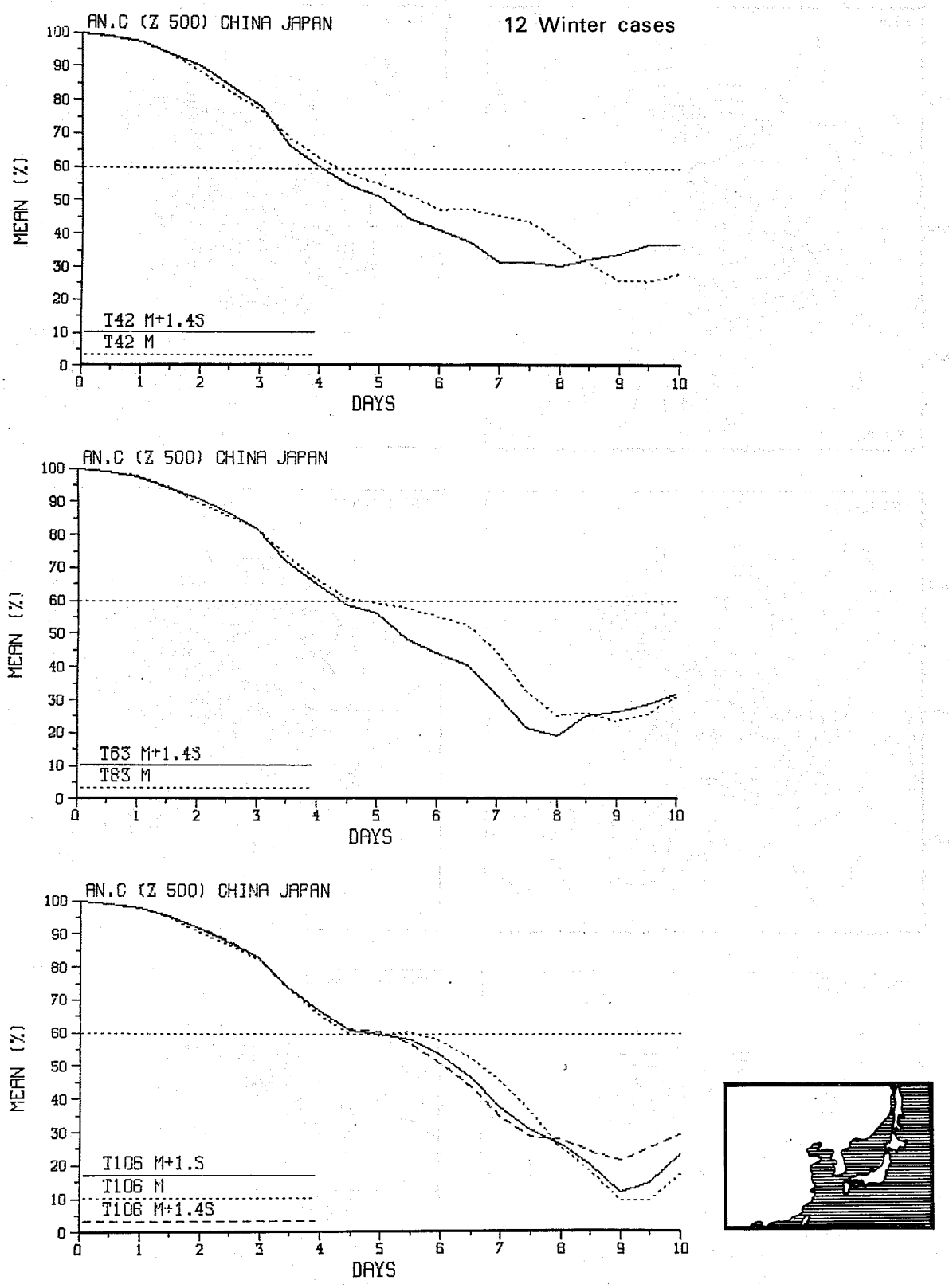

Fig.14 Mean anomaly correlations of 500 mb height field averaged over 12 winter cases for the region 100°E to 150°E and 20°N to 55°N at T42, T63 and T106 resolution (from top to bottom) using mean or envelope orographies.

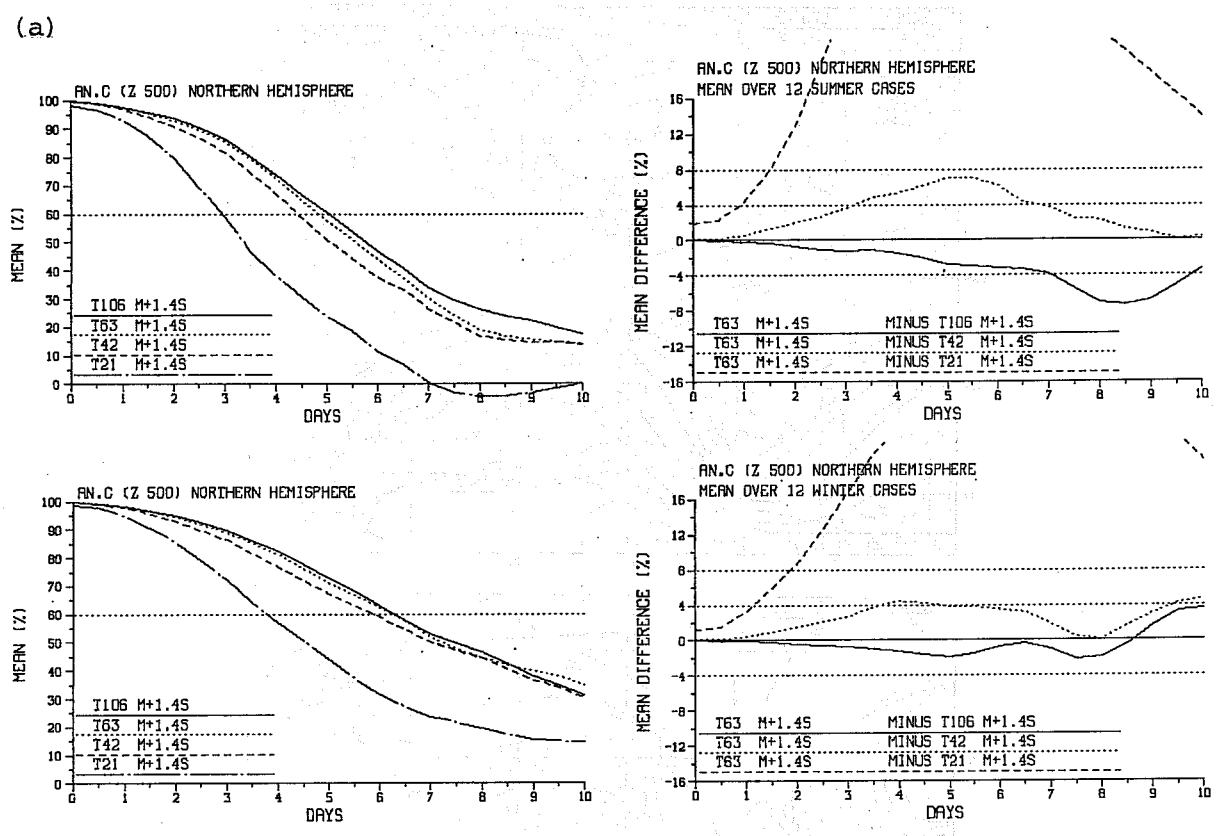

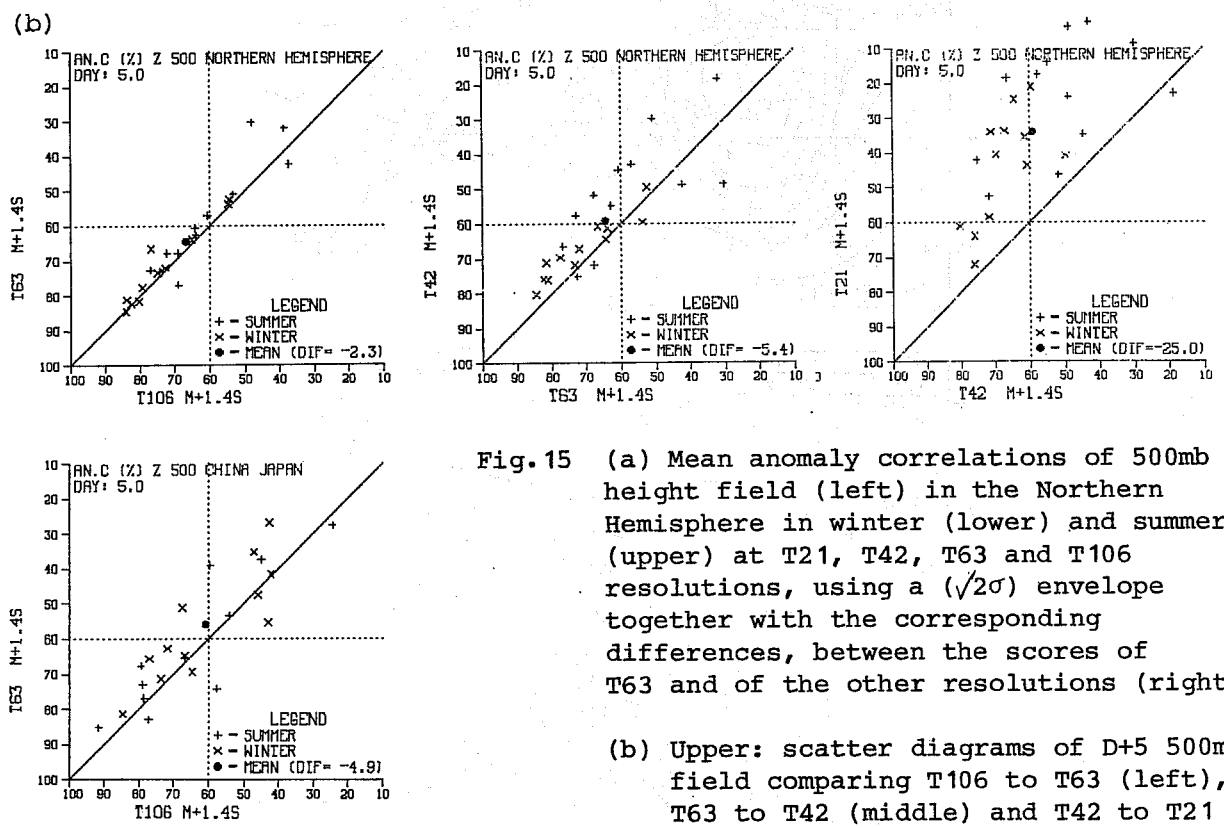

Fig. 15 (a) Mean anomaly correlations of 500mb height field (left) in the Northern Hemisphere in winter (lower) and summer (upper) at T21, T42, T63 and T106 resolutions, using a ($\sqrt{2}\sigma$) envelope together with the corresponding differences, between the scores of T63 and of the other resolutions (right)

(b) Upper: scatter diagrams of D+5 500mb field comparing T106 to T63 (left), T63 to T42 (middle) and T42 to T21 (right)

Lower: similar diagram comparing T106 and T63 over the China-Japan area, defined in Fig. 14.

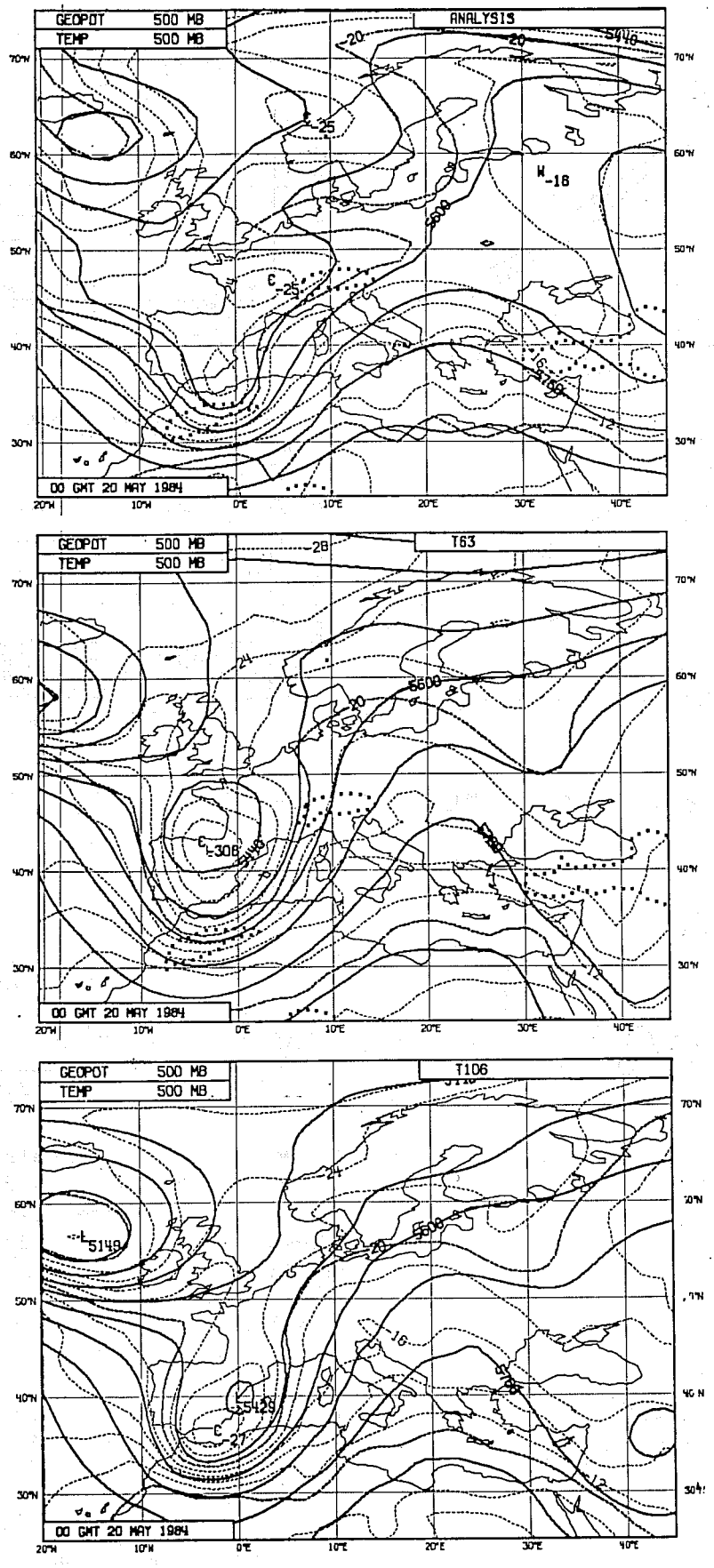

Fig. 16 Analysed 500 mb height and temperature fields for 20 May 1984 over Northern Atlantic and corresponding T63 and T106 D+5 forecasts using a ($\sqrt{2}\sigma$) envelope.

ECMWF/SAC(85)4

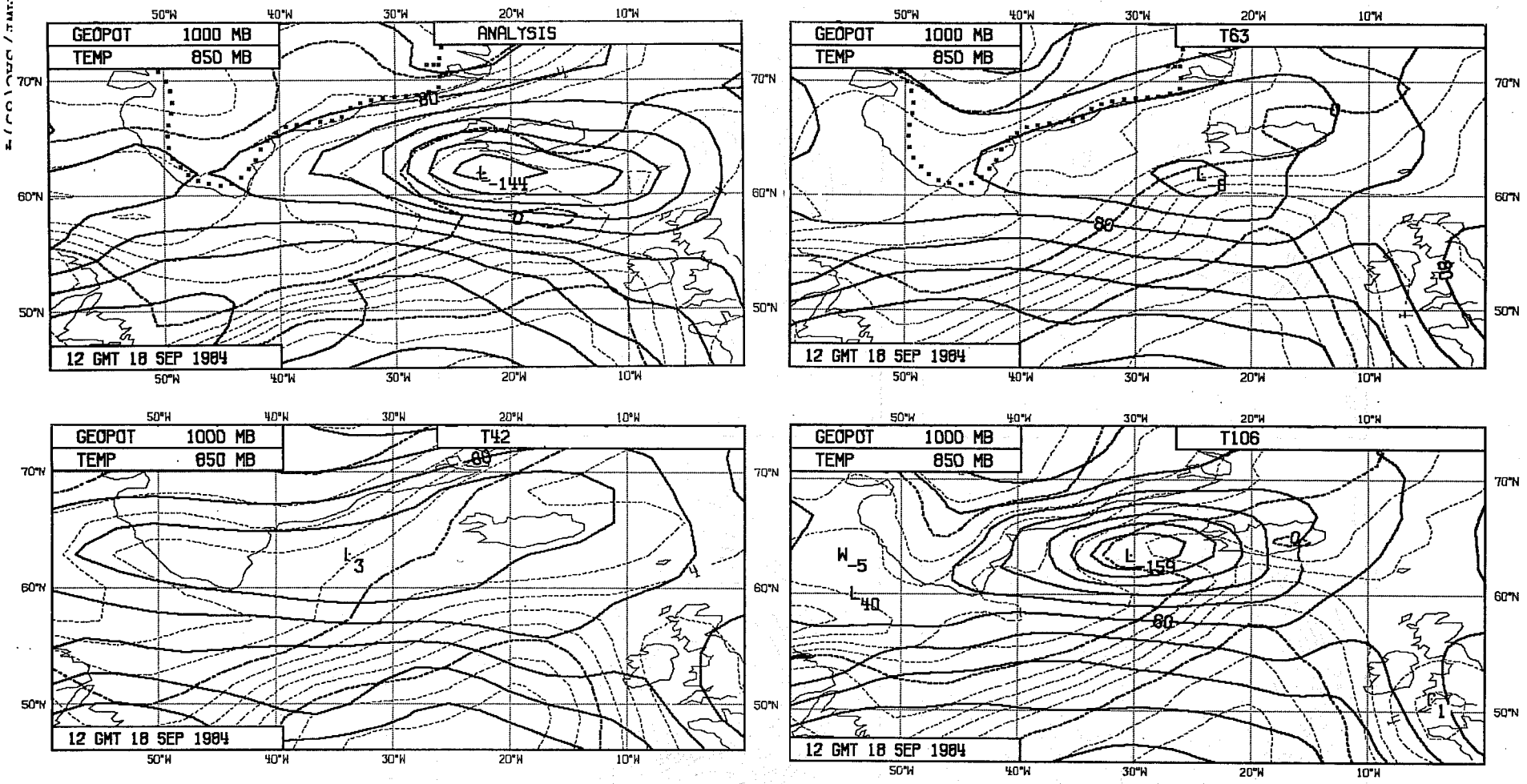

Fig. 17 Analysed 1000 mb height and 850 mb temperature fields for 18 Sept. 1984 over Northern Atlantic and corresponding T42, T63 and T106 D+3 forecasts using a ($\sqrt{2}\sigma$) envelope.

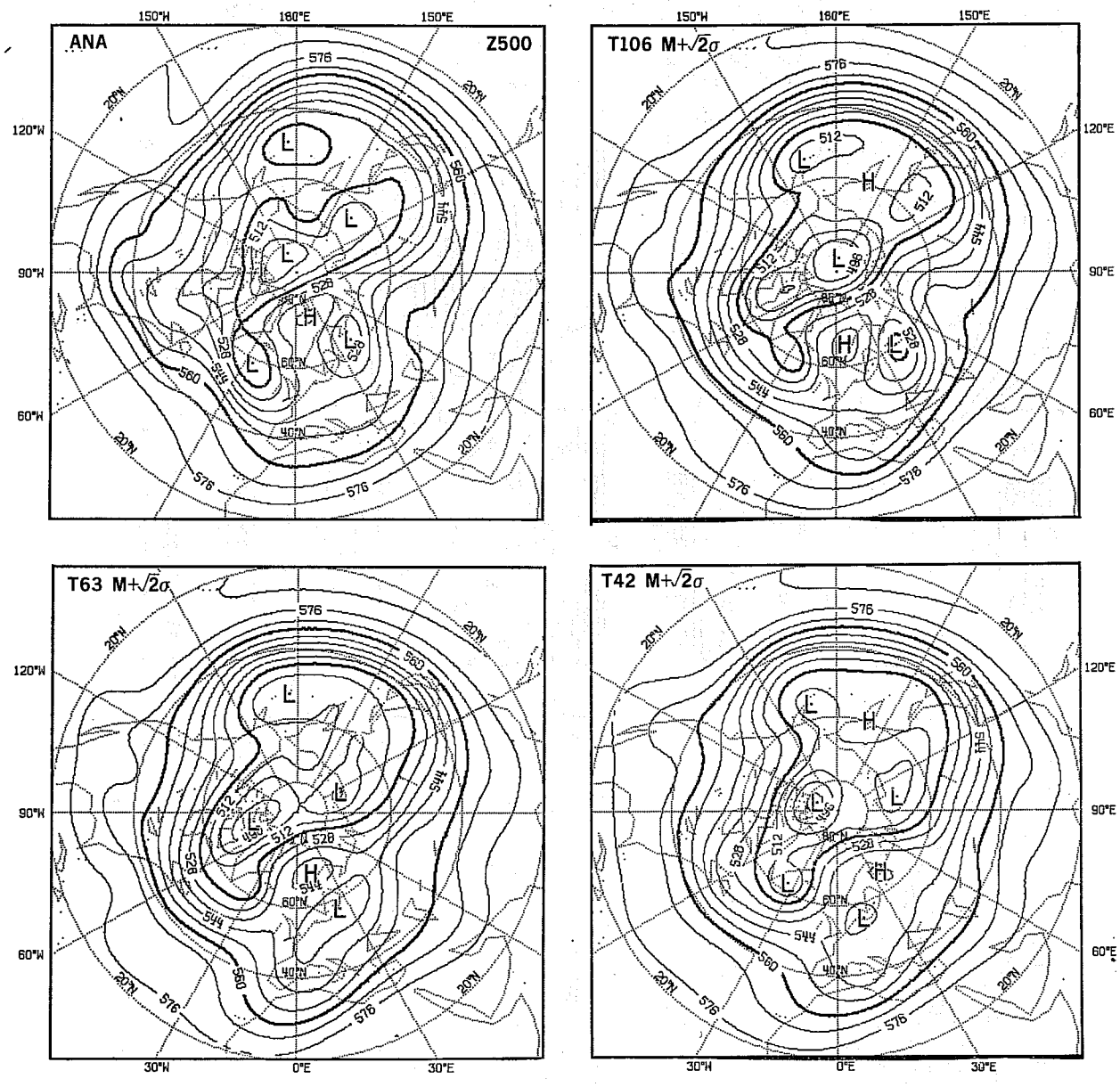

Fig.18 Analysed maps of 500 mb height field averaged over the period 20h 25 March 1984 and corresponding D+5 to D+10 mean maps of forecasts by T42, T63 and T106 using a ($\sqrt{2}\sigma$) envelope.

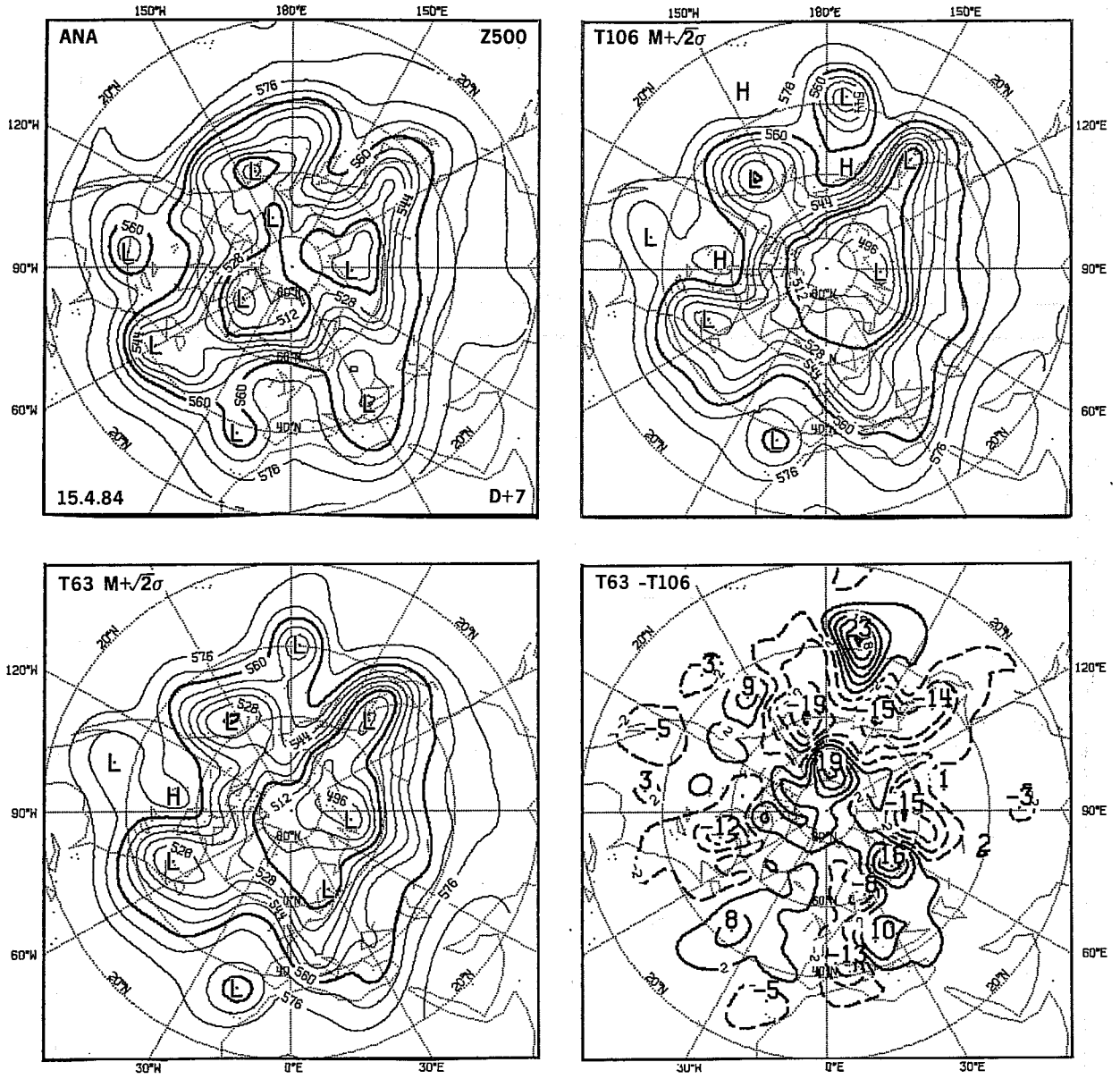

Fig. 19 Analysed 500 mb height field for 22 April 1984 and corresponding D+7 T106 and T63 forecasts using a ($\sqrt{2}\sigma$) envelope together with the associated difference map.

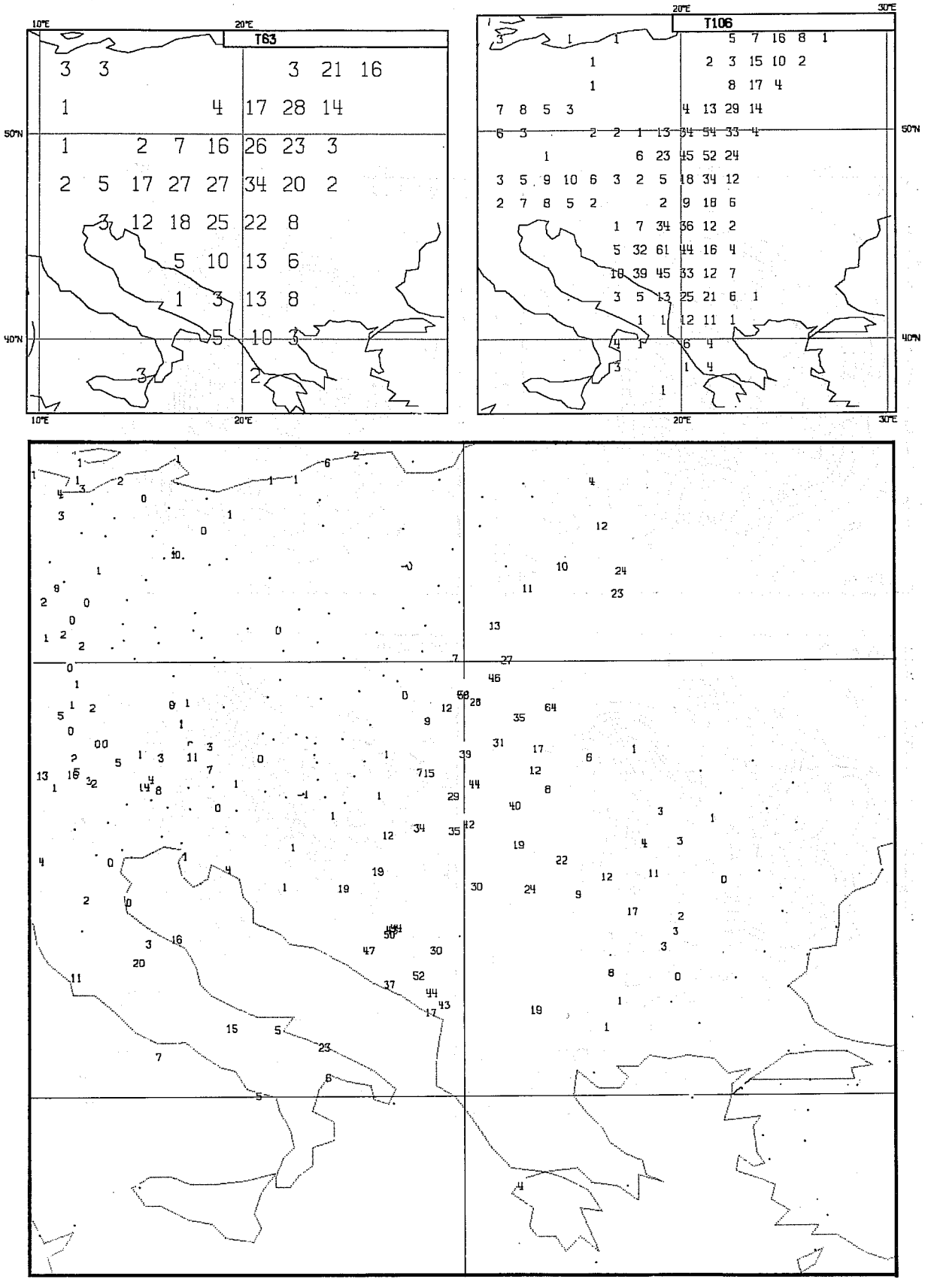

Fig.20 Precipitation totals (mm) between days 2 and 3 of T63 (upper left) and T106 (upper right) forecasts from 15 September 1983, and corresponding observed values (lower map). Forecast values are plotted at each grid point where the precipitation exceeded 1 mm. Observations of no precipitation are represented by a dot, and a zero denotes that a trace was observed.

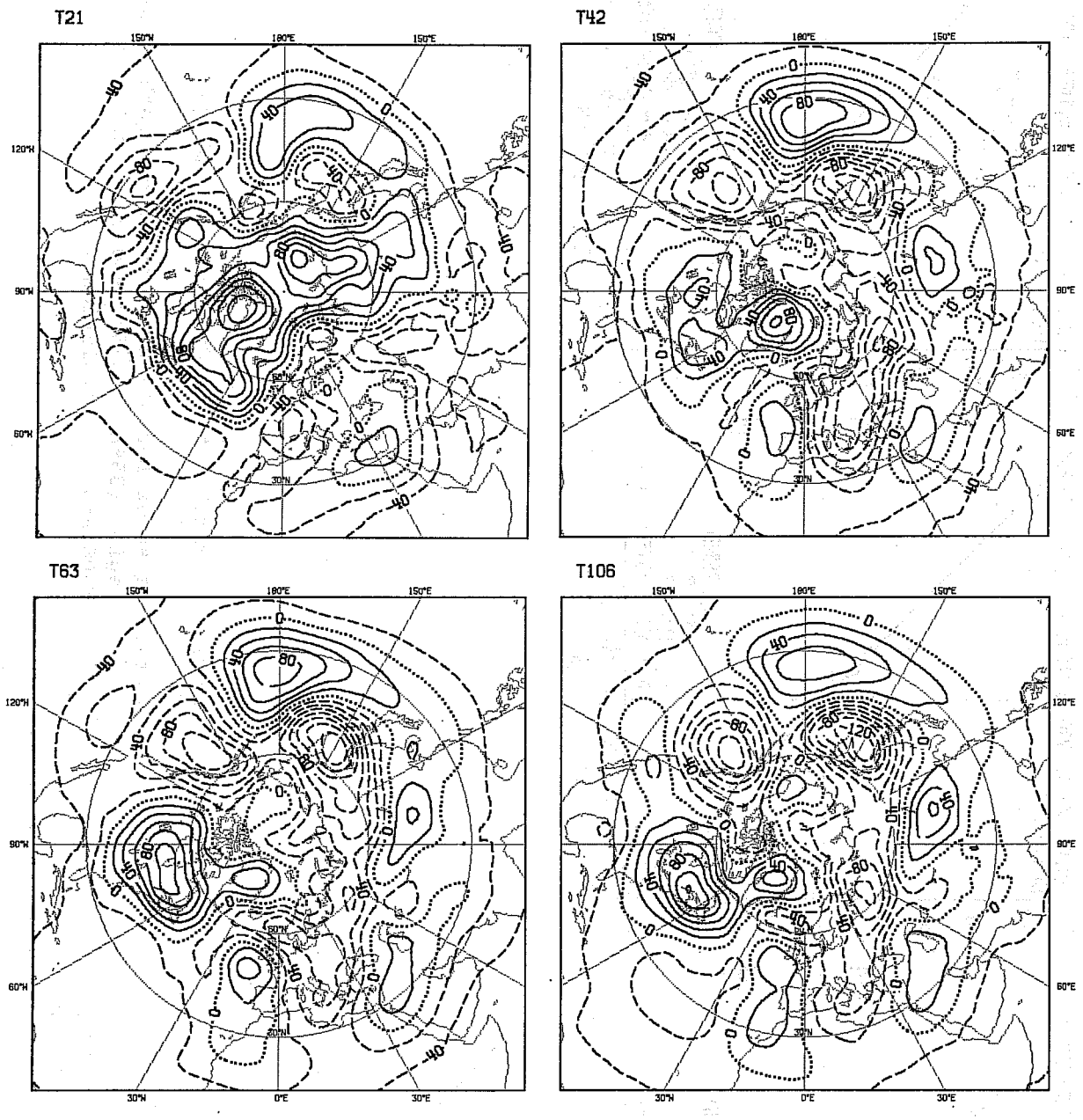

Fig.21 Errors in the 500 mb height field averaged over days 8, 9 and 10 and the 12 "winter" cases, for T21, T42, T63 and T106 forecasts. Positive contours are solid, and negative contours dashed. The contour interval is 20 m.

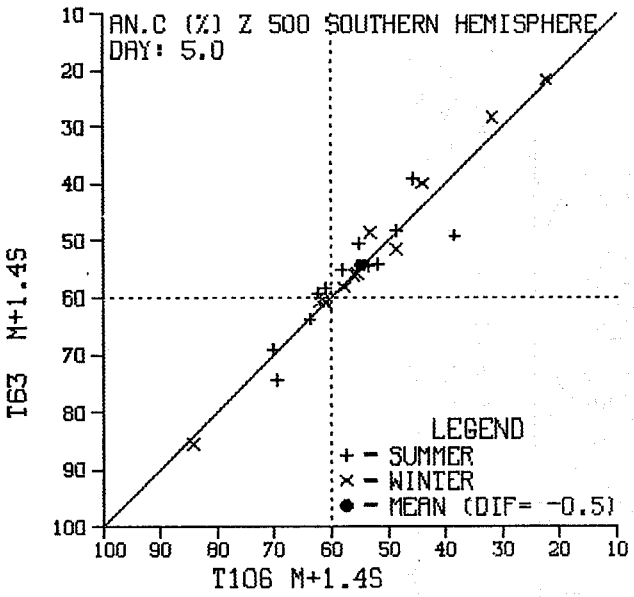

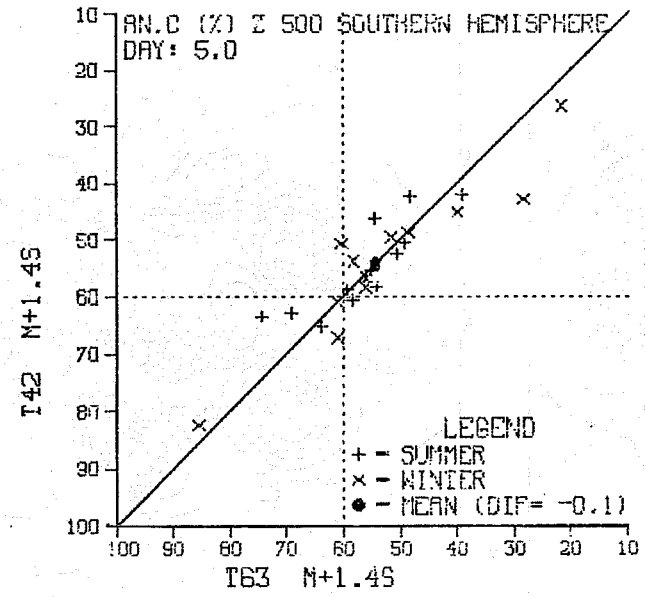

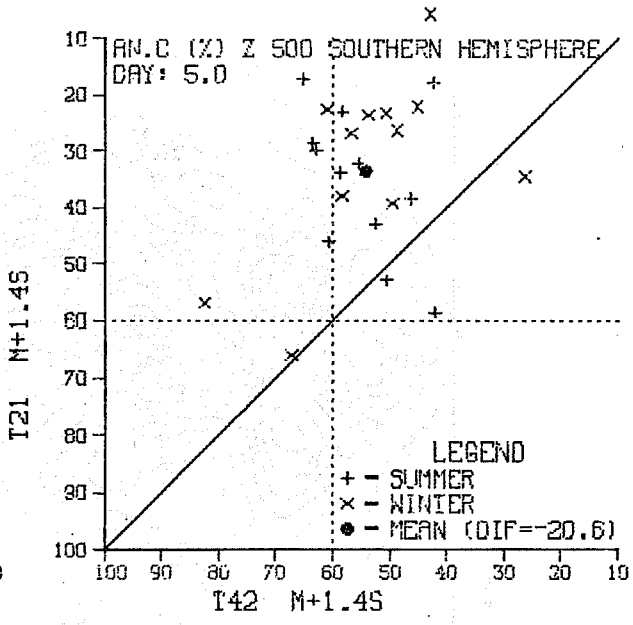

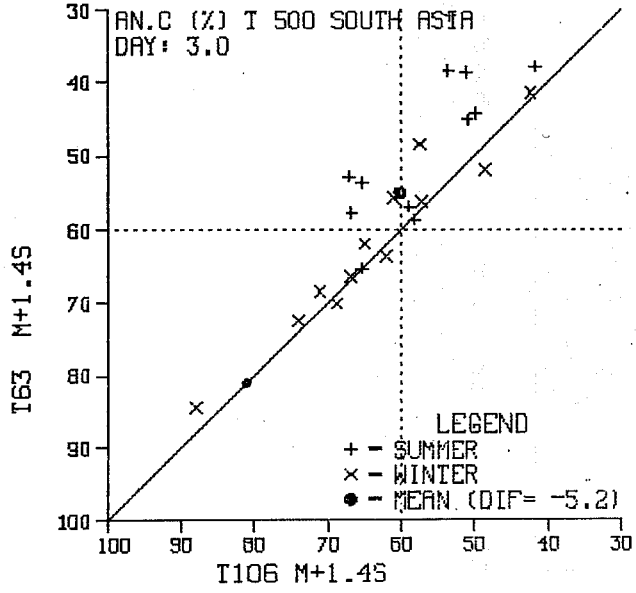

Fig.22 (Upper): As Fig.9 but for Southern Hemisphere.

(Lower): As above for D+3 forecasts over South Asian region (35°E to 125°E and 0° to 30°N) for T106 and T63 resolutions.

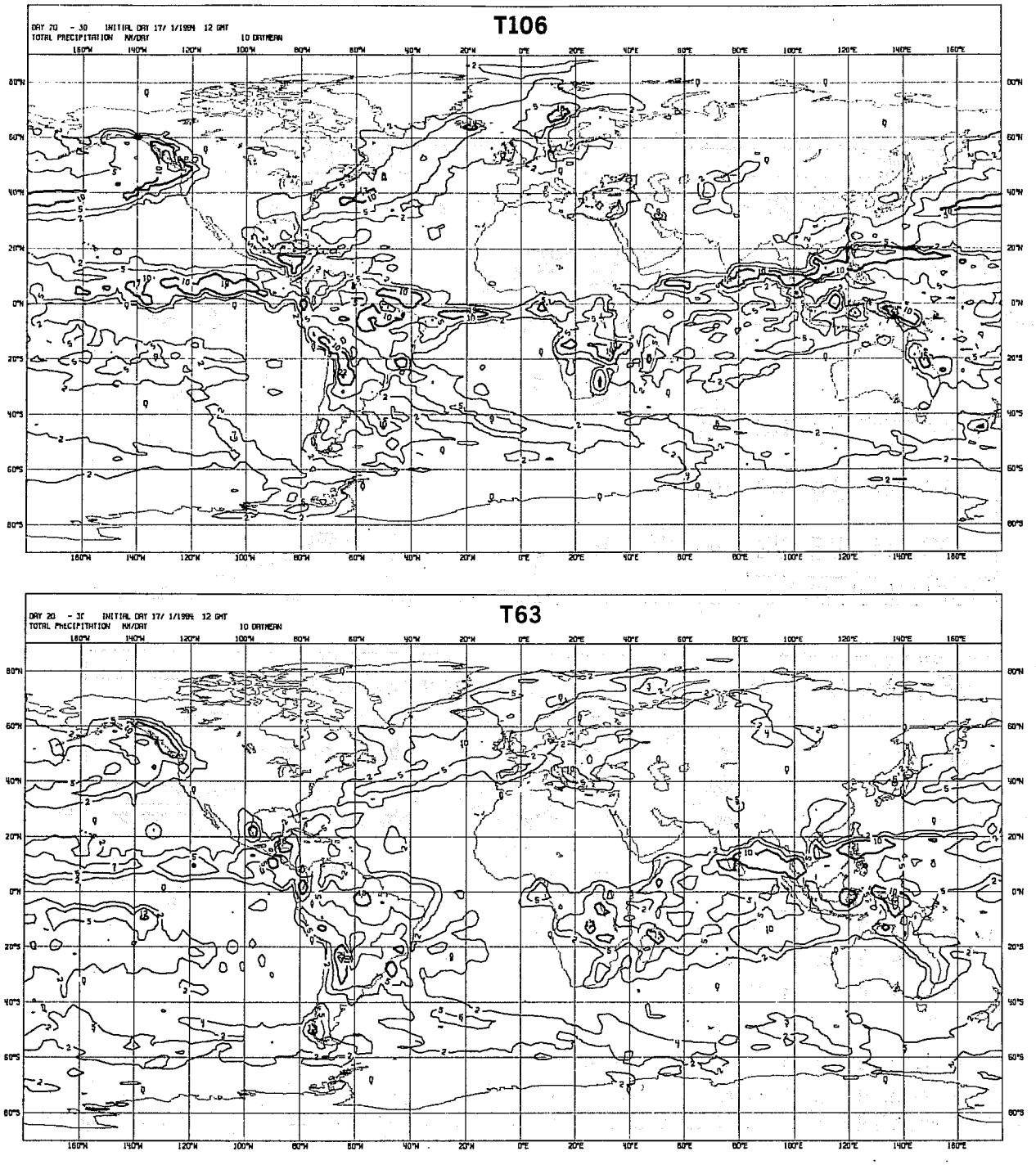

Fig.23 Precipitation rates (mm/day) averaged over the last 10 days of 30-day T106 (upper) and T63 (lower) integrations starting from 17 January 1984.

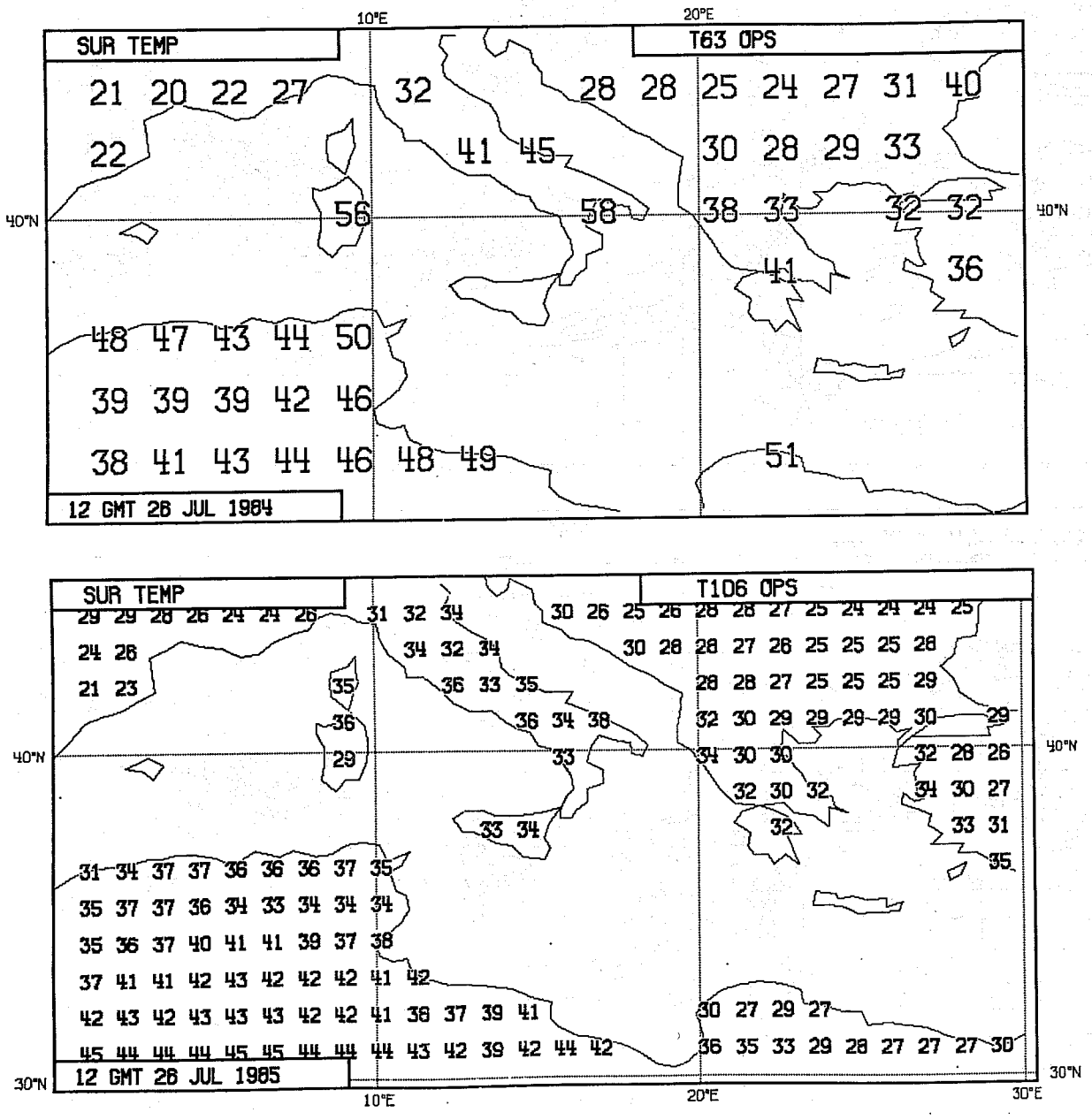

Fig.24 The D+3 operational T63 forecast of land surface temperature for 26 July 1984, and the T106 operational forecast carried out one year later.

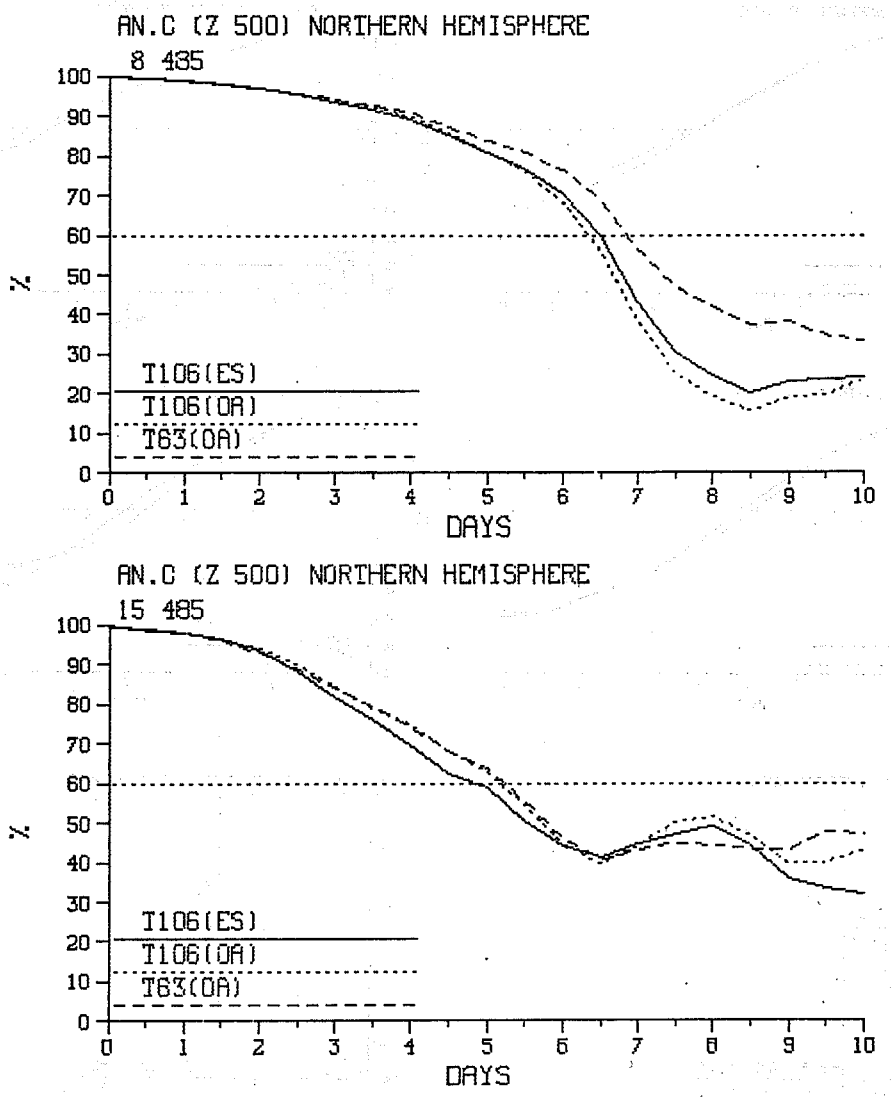

Fig.25 Anomaly correlations of 500 mb height for Northern hemisphere for forecasts from 8 and 15 April 1985. The solid curves denote T106 results using the trial analyses as initial data, and the dotted curves T106 results using interpolated, operational T63 analyses. T63 forecasts from the latter analyses are denoted by the dashed curves.

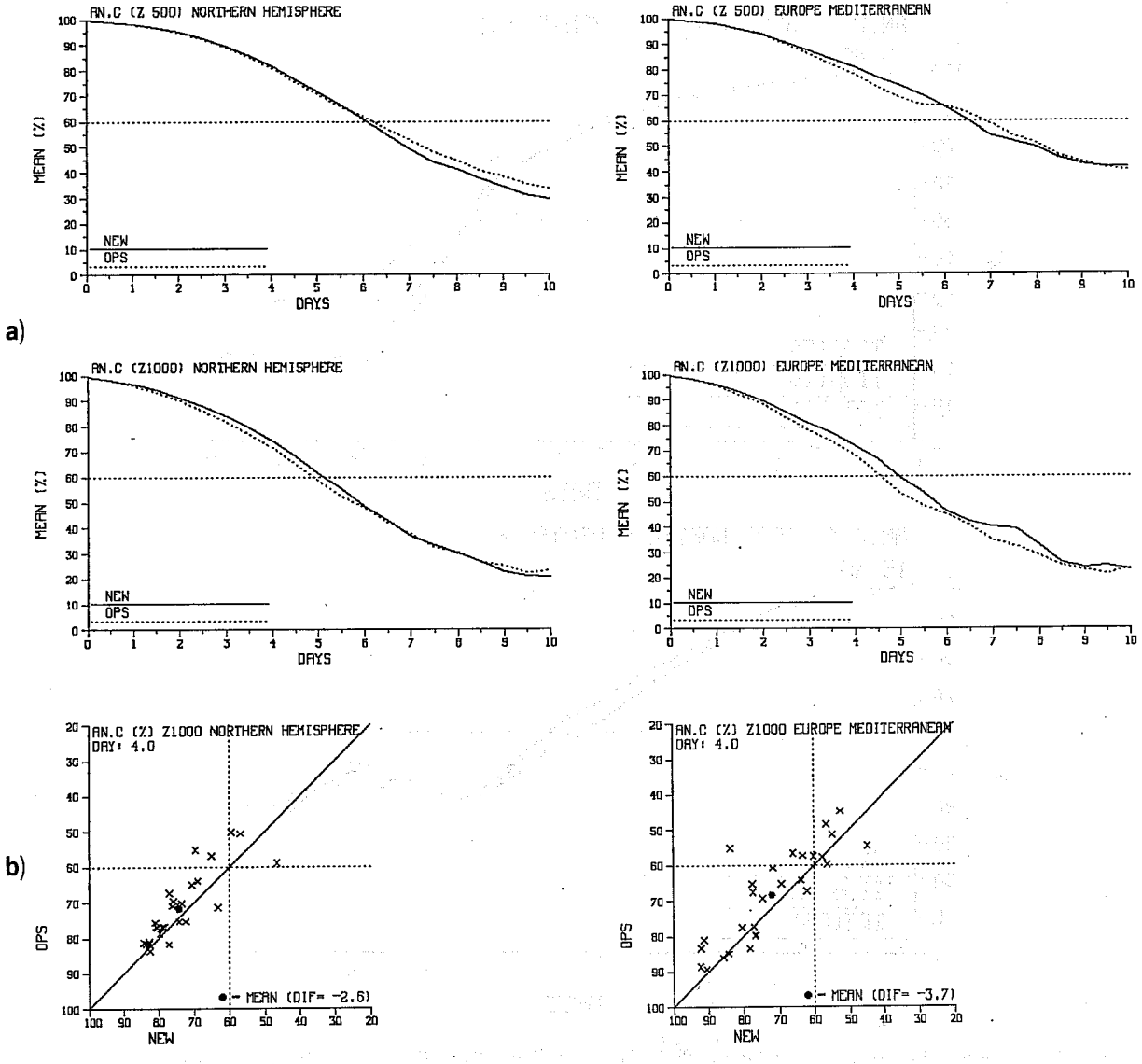

Fig.26 (a) Mean anomaly correlation of 500 mb (upper) and 1000 mb (lower) height for the Northern Hemisphere (left) and over Europe and the Mediterranean 30°-75°N, 20°W-45°E (right). The solid lines denote results from the trial forecasts with the revised model; operational forecasts are denoted by the dotted curves.

(b) Scatter diagrams of anomaly correlations of 1000 mb height comparing D+4 trial (labelled NEW) and operational (labelled (OPS) forecasts for the Northern Hemisphere and over Europe and the Mediterranean.

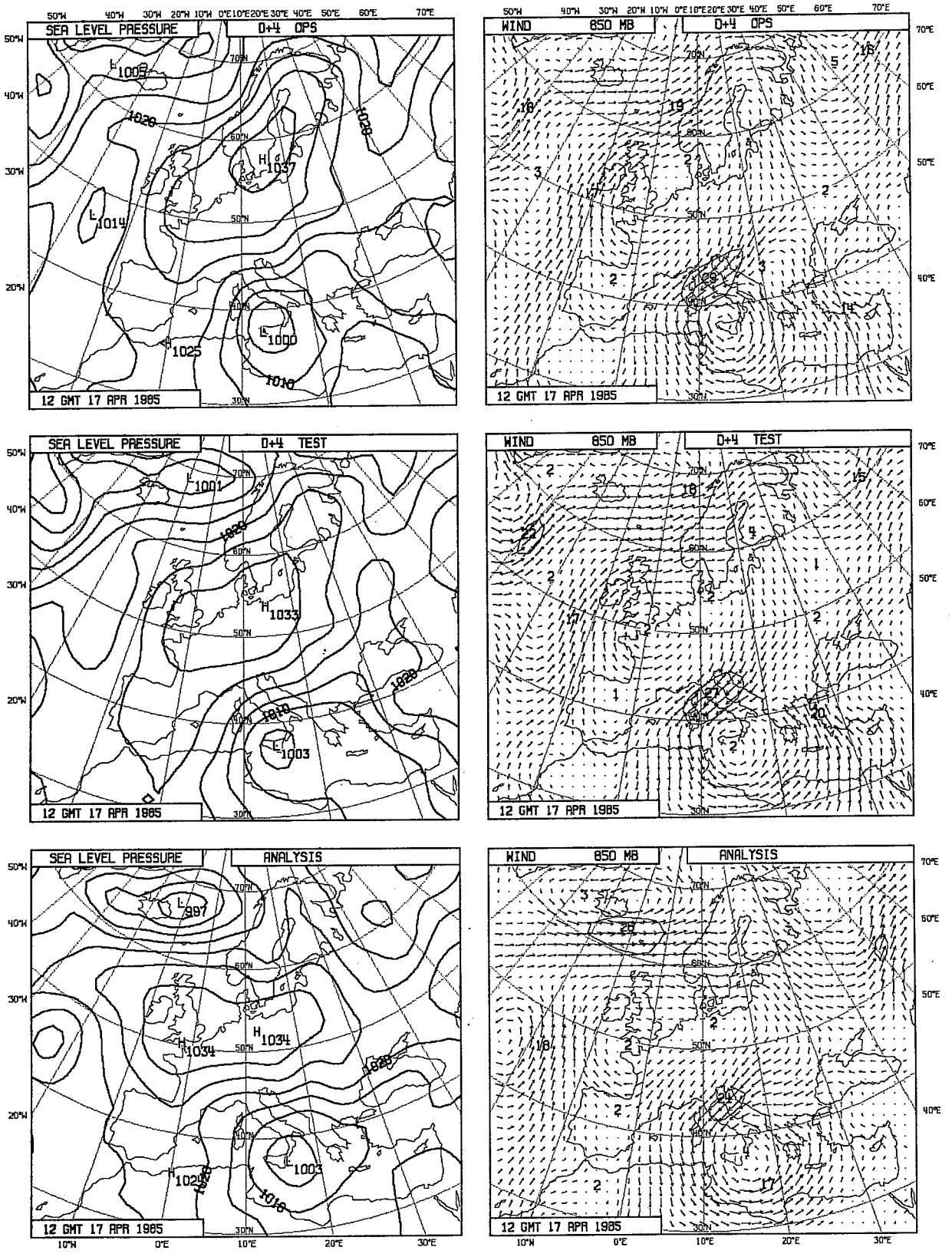

Fig.27 Operational (upper) and trial (middle) D+4 forecasts of mean sea-level pressure and 850 mb wind over Europe, and the corresponding verifying (operational) analyses (lower).